BEHAVIOR OF COMPOSITE BEAMS WITH WEB OPENINGS

by

KRIGO S. ELIUFOO

B.S., Kansas State University, 1978

A MASTER'S THESIS

submitted in partial fulfillment of the

requirements for the degree

MASTER OF SCIENCE

Department of Civil Engineering

KANSAS STATE UNIVERSITY
Manhattan, Kansas

1979

Approved by:

Stuart E Swartz

Major Professor

TABLE OF CONTENTS

LIST OF FIGURES

LIST OF TABLES

INTRODUCTION

In the design of high-rise structures, especially steel building frames, steel beams with web openings are commonly used. These openings are used for locating utility ducts rather than placing them below the steel beams and girders. By doing this the total building height is reduced significantly and a more economical design is achieved.

In recent years many studies of these beams have been made by a number of investigators, leading to methods of their analysis and design. However, a related problem of some significance which to date has not been studied in great detail is the steel-concrete composite beam with web openings. In the first section of this report a complete elastic analysis of composite beams with web openings is presented. The problem was approached using standard assumptions of elastic behavior of a transformed section with application of the Vierendeel Method of analysis. In the second section of this report some considerations for ultimate strength analysis of the same beams are presented.

For both analyses a sufficient number of shear connectors are assumed to be present so that full composite action is attained. The openings are assumed to be rectangular and unreinforced.

ELASTIC ANALYSIS

Assumptions

The following assumptions were made in this analysis.

1. A point of contraflexure occurs at the midpoints of the sections above and below the opening (Vierendeel action).

2. Shear, which causes secondary bending, is constant along the length of the hole. Only the uncracked portion of the slab carries shear.

3. The deflection curve of the section above the hole is identical to that below the hole as assumed by Knostman, et al. (1).

Solution Outline

The solution to this problem has been approached in a simple manner and by basically adhering to the assumptions of beam bending theory.

In solving the problem the section properties are first defined. Then a consideration of equilibrium of forces and moments on a transformed cracked section (Fig. 1) leads to the general stress equations. The concrete is assumed cracked at some depth c_r below the surface of the slab. By applying the requirement of zero stress at the cracked surface an equation for c_r is obtained. By using the assumptions made by Knostman, et al. (1), in particular, that the deflection curve of the section above the hole is identical to that below the hole, a relationship between the top shear force V_T, and the bottom shear force V_B is obtained.

With the above information the normal service stresses can be computed by a trial and error procedure for any location along the length of the hole. A fairly short computer program has been written to facilitate this process.

Section Properties

Referring to Fig. 1, the cross-section properties are defined as follows:

Top composite area, $A_T = b_s c_r + A_{Ts}$.

Top steel area, $A_{Ts} = bt + s_T t_w$.

Bottom steel area, $A_B = bt + s_B t_w$.

Net cross-section area, $A = A_T + A_B$.

Top steel centroid,

$$\bar{s} = [\tfrac{1}{2} bt^2 + s_t t_w (\tfrac{1}{2} s_T + t)]/A_{Ts}. \quad (1)$$

Top steel moment of inertia,

$$I_{Ts} = \tfrac{1}{12} bt^3 + bt (\bar{s} - \tfrac{1}{2} t)^2 + \tfrac{1}{12} t_w s_T^3 + s_T t_w (\tfrac{1}{2} s_T + t - \bar{s})^2. \quad (2)$$

Top composite centroid,

$$\bar{y}_T = [\tfrac{1}{2} b_s c_r^2 + A_{Ts} (\bar{s} + c)]/A_T. \quad (3)$$

Bottom centroid,

$$\bar{y}_B = [s_B t_w (\tfrac{1}{2} s_B + t) + \tfrac{1}{2} bt^2]/A_B. \quad (4)$$

Centroid of composite section,

$$\bar{y}_N = [A_B (d - \bar{y}_B + c) + A_T \bar{y}_T]/A. \quad (5)$$

Moment of inertia of composite top section,

$$I_T = \tfrac{1}{12} b_s c_r^3 + b_s c_r (\bar{y}_T - \tfrac{1}{2} c_r)^2 + I_{Ts} + A_{Ts} (\bar{s} + c - \bar{y}_T)^2. \quad (6)$$

Moment of inertia of bottom section,

$$I_B = \frac{1}{12} t_w s_B^3 + s_B t_w \left(\frac{1}{2} s_B + t - \bar{y}_B\right)^2 + \frac{1}{12} bt^3 + bt \left(\bar{y}_B - \frac{1}{2} t\right)^2. \quad (7)$$

Moment of inertia of composite section,

$$I_N = I_B + A_B (d - \bar{y}_B + c - \bar{y}_N)^2 + I_T + A_T (\bar{y}_N - \bar{y}_T)^2. \quad (8)$$

In the above equations if the section is uncracked, replace c_r by c.

Shear Ratio, V_T/V_B

By equating the deflections of the top and bottom sections at the center of the opening and considering both shearing and bending deflections the ratio V_T/V_B can be shown to be

$$\frac{V_T}{V_B} = \frac{\frac{a^2 G}{3 I_B E} + \frac{K_B}{A_B}}{\frac{a^2 G}{3 I_T E} + \frac{K_T}{A_T}} \quad (9)$$

as derived by Knostman, et al. (1). In this equation a is the half-length of the hole, E and G are the modulus of elasticity and modulus of rigidity for steel. A_T, A_B and I_T, I_B are transformed areas and moments of inertia above and below the hole. $V_T + V_B = V$ is the applied shear at the section. The terms K_T, K_B are section shape factors for shear deformation, and are determined in Appendix III.

Elastic Stresses and Neutral Axis Location

The general service stress equations for the top and bottom sections are:

$$f_T = \frac{M_P y_N}{I_N} + \frac{V_T \times y_T}{I_T} \quad \text{---------- (10a)}$$

$$f_B = \frac{M_P y_N}{I_N} + \frac{V_B \times y_B}{I_B} . \quad \text{---------- (10b)}$$

These equations are derived by considering the equilibrium of forces and moments on a transformed, cracked section shown in Fig. 1. The term y_N is the distance from the neutral axis of the section to the location where the stress is desired and similarly y_T, y_B are the distances from the neutral axes of the top and bottom sections. M_P is the moment at the center of the opening and x is the distance from the center of the opening to any location of interest along the opening as shown in Fig. 2 ($-a \leq x \leq a$).

In order to locate the neutral axes of the top and net sections the value of c_r must be known. This is some depth below the top surface to where the concrete has cracked due to tensile stress. From this depth to the bottom of the slab, the concrete stress is zero due to the assumption that no concrete tensile stress can exist in a cracked section.

Note that this implies cracking proceeding from the bottom of the slab such as could occur at the high moment edge of the hole. The other possibility is cracking proceeding from the top surface downward, as could occur at the low moment edge. This immediately leads to a conclusion that the entire section is cracked. This will have to occur in order to satisfy statics because of the assumption that no concrete tensile stress can exist in a cracked section.

Applying the requirement of zero stress in the concrete leads to

$$c_r = \frac{\frac{M_T \bar{y}_T}{I_T} + \frac{M_P \bar{y}_N}{I_N}}{\frac{M_T}{I_T} + \frac{M_P}{I_N}} \qquad \text{(11)}$$

where, $M_T = V_T x$. Expressions for $\bar{y}_T$, $\bar{y}_N$, I_T, I_N are as were given previously.

Method of Solution

In solving for the parameter c_r by expanding Eq. (11), a fairly complicated polynomial of c_r results because $\bar{y}_T$, $\bar{y}_N$, I_T, I_N and M_T all contain the parameter c_r. A more suitable method to determine c_r is by trial and error. In this method a value of c_r is assumed, normally the full slab depth c. Experience with a number of numerical examples has shown that convergence within an error tolerance of 1% occurs very rapidly with the starting value of c_r equal to c.

Since the algebraic expressions which must be evaluated at each iteration are lengthy, a fairly short computer program written in Fortran was developed to facilitate the iteration process. This program initially assumes a value for $\alpha = V_T/V$ (= 0.9) and c_r (= c). With α fixed, the program determines a value for c_r by an iteration process. The equations for K_T and K_B in Appendix III are then employed to compute a new value for α. Using this new value for α, again a convergence for c_r is obtained. This procedure is repeated until convergence is obtained for both α and c_r. Then using the general service stress equations, stresses are computed for the locations shown in Fig. 3 from which the top and bottom horizontal forces are obtained. The stress equations for the locations shown in Fig. 3 are shown in Appendix IV. The flow diagram for the computer program developed in this report is shown in Fig. 3a.

If the cracking proceeds from the top downward, the value of c_r is set to zero. It is assumed all the concrete cracks and is not effective. The ratio α for the resulting steel section is computed directly, and the stresses obtained for the locations shown in Fig. 3 by using the stress equations given in Appendix IV.

Shear Carried by Concrete

The area of the concrete slab as compared to the area of the top steel section is normally large, especially if the concrete is uncracked. It is thus of interest to know the amount of shear carried by the concrete. The shear stress v_c in the concrete portion of the transformed section above the hole is obtained following the classical bending theory. That is,

$$v_c = \frac{V_T Q_c}{n I_T b_s} \qquad (12)$$

in which Q_c is the first area moment about the top neutral axis (See Fig. 4a). The division by n in Eq. (12) is to convert the current steel stress into concrete stress.

By directly integrating Eq. (12) over the uncracked portion of the slab, the ratio V_{Tc}/V_T can easily be shown to be

$$\frac{V_{Tc}}{V_T} = \frac{b_c c_r^2 (3\bar{y}_T - c_r)}{6 n I_T} \qquad (13)$$

From Eq. (13) it can be noted that the ratio V_{Tc}/V_T will remain constant along the length of the hole, provided the concrete remains uncracked. c_r, $\bar{y}_T$ and I_T in Eq. (13) will be constant along the length of the hole if this occurs. The assumption that shear in the concrete is carried by the uncracked portion only is conservative, for some

shear will be carried in the cracked section because of aggregate interlock on cracked surfaces and because of the reinforcing steel.

Examples

Three beams were analyzed by the method described in this report and also using a finite element computer program (3) with the capability of utilizing non-linear material properties and cracking in the concrete. The properties of the three beams are presented in Table 1 and Fig. 5.

The beams were loaded as shown in Fig. 5 and the stresses obtained by the two methods were plotted. For each beam the stresses at the high and low moment edges of the hole were plotted as well as for some other sections in between. In all cases there was a reasonable agreement between the two methods. The plots are shown in Figs. 6, 7 and 8.

The stresses obtained for Beam No. 3 by using the method presented in this report were appropriately converted to strains and compared to actual experimental test results.[1] Beam No. 3 was loaded as shown in Fig. 5 in the test and electric resistance strain gages were used to measure the surface strains. The results obtained were plotted and are shown in Fig. 9. Again the calculated results were in a fairly good agreement with the test results.

The shear ratios V_T/V and V_{Tc}/V obtained by the method developed in this report and by the finite element program (3) for the three beams are shown in Table 2. A reasonable agreement between the two methods is again shown.

It should be noted that in all the examples presented here the selfweight of the beams were neglected.

---

[1]The experimental data was obtained from tests conducted at the University of Kansas.

CONSIDERATIONS FOR ULTIMATE STRENGTH ANALYSIS

General Assumptions

The general assumptions made in this consideration are the following:

1. At the point of contraflexure the axial (normal) stress is zero for the case of secondary moment only.

2. Shear, which causes secondary bending is constant along the length of the hole.

3. Shear in the steel section is carried by the areas $t_w(s_b + t)$ for the bottom section and $t_w(s_t + t)$ for the top section, and is uniformly distributed.

4. The Von Mises Failure Law is assumed for the steel.

5. A linear failure law is assumed for the concrete (2).

6. Failure due to instability and the effects of strain hardening are not considered.

7. Equilibrium and compatibility are satisfied.

Failure Laws

The Von Mises Failure Law for the steel may be written as:

$$f_v = \sqrt{\frac{1}{3}(f_y^2 - f_s^2)} \qquad \text{(14)}$$

in which f_v is the shearing stress, f_y the yield stress and f_s the normal stress.

The Linear Failure Law for the concrete is derived by considering the interaction diagram (2) shown in Fig. 10 and Mohr's circle of stresses constructed for concrete. The equation for the linear portion of Fig. 10 is

$$\sigma_2 = -f_c' + \frac{f_c'}{f_t'}\sigma_1 \qquad \text{(15a)}$$

where σ_1 and σ_2 are the principle stresses, f_c' and f_t' are the compressive and tensile strengths of concrete.

From Mohr's circle of stresses for concrete the principle stresses can easily be shown to be

$$\sigma_1, \sigma_2 = -\frac{1}{2} f_c \pm \sqrt{\frac{1}{4} f_c^2 + f_{vc}^2} \quad \text{---------- (15b)}$$

in which f_c and f_{vc} are the compressive and shearing stresses of concrete.

The following equation is obtained by equating equations (15a) and (15b)

$$\sqrt{\frac{1}{4} f_c^2 + f_{vc}^2} = \frac{2 f_c' f_t' + f_c(f_c' - f_t')}{2 (f_c' + f_t')} .$$

Simplifying and solving for f_{vc} leads to the form in which the equation is desired,

$$f_{vc} = \frac{1}{2}\sqrt{f_c' f_t' \left[1 - \left(\frac{2 f_c - f_c' + f_t'}{f_c' + f_t'}\right)^2\right]} \quad \text{---------- (16)}$$

Equation (16) is the Failure Law for concrete as used in this report.

Discussion of Approach

There are two principle cases in the approach used here. In case a the ultimate moment at the center of the hole M_u is assumed zero and the amount of shear V_u the beam can carry in the region of the hole is determined. This shear is determined at the critical locations, that is at the edges of the opening where the secondary moment (moment due to shear) is maximum. Simple assumptions are made to facilitate the development of equations and these assumptions are later modified and made more realistic in two steps. The assumptions and equations developed in the three steps are referred to as Models 1, 2 and 3.

In the first model the concrete is assumed to carry tension at failure ($f_t = f_c$) and the shearing stress f_{vc} is assumed to be carried by the entire concrete section. Using these assumptions the normal stress distribution at the low moment edge will be exactly equal and opposite to the normal stress distribution at the high moment edge. For equilibrium of forces to be attained, the point of contraflexure will have to occur at the center of the opening.

In the second model the amount of tension the concrete can carry is reduced and is assumed to be $f_t = \gamma f_c$. The factor γ is some number less than one, but not equal to zero. The shearing stress f_{vc} is still assumed to be carried by the entire concrete section. In the third model it is assumed, $f_t = \gamma f_c$ and the shearing stress f_{vc} to be carried in the compressed portion of the concrete section only.

For case b, the ultimate moment M_u is assumed not to be zero. Some known ratio, $\theta = M_u/V_u$ is assumed and the process described previously is followed in determining the ultimate moment and shear.

In this report the equations of Model 1 for both cases a and b have been developed. For case a, the shear capacity V_u for Beams 1, 2 and 3 were determined using the equations developed. The results obtained appeared high when compared to test results. This was expected because of the assumption, $f_t = f_c$.

Some interesting conclusions were reached for the second model case a while attempting to develop the equations. These conclusions are also presented.

The results of evaluating Models 1 and 2 led to modifications which resulted in the proposed third model as stated above.

Development of Equations

Model 1, Case a

Only one neutral axis was assumed in the top section and one in the bottom section for all cases and models as determined from the elastic analysis. Two sets of equations were developed. The first for the case when the top neutral axis (NA_T) and the bottom neutral axis (NA_B) are in the steel flanges and the second for the case when the top neutral axis is in the concrete slab and the bottom neutral axis is in the web.

At the outset the failure laws for the concrete, the top steel section and the bottom steel section may be written as:

$$f_{vc} = \frac{1}{2}\sqrt{f_c' f_t'}\left[1-\left(\frac{2f_c - f_c' + f_t'}{f_c' + f_t'}\right)^2\right]$$

$$f_{vT} = \sqrt{\frac{1}{3}\left(f_y^2 - f_{sT}^2\right)}$$

$$f_{vB} = \sqrt{\frac{1}{3}\left(f_y^2 - f_{sB}^2\right)}$$

where f_{vT} and f_{vB} are the shearing stresses in the top and bottom steel sections, f_{sT} and f_{sB} are the normal stresses in the top and bottom steel sections.

Referring to Fig. 11, the total shear carried by the concrete slab,

$$V_c = \frac{cb_c}{2}\sqrt{f_c' f_t'}\left[1-\left(\frac{2f_c - f_c' + f_t'}{f_c' + f_t'}\right)^2\right] \qquad \text{(17)}$$

The total shear carried by the top steel section,

$$V_{sT} = A'_{sT}\sqrt{\tfrac{1}{3}(f_y^2 - f_{sT}^2)} \quad \text{---------- (18)}$$

in which $A'_{sT} = t_w(s_T + t)$.

The total shear carried by the bottom steel section,

$$V_{sB} = A'_{sB}\sqrt{\tfrac{1}{3}(f_y^2 - f_{sB}^2)} \quad \text{---------- (19)}$$

in which $A'_{sB} = t_w(s_B + t)$

Hence, the total amount of shear the section can carry,

$$V_u = V_c + V_{sT} + V_{sB} \quad \text{---------- (20)}$$

In Fig. 11, independent consideration of the equilibrium of forces of the three free body diagrams and their moments about points A and B leads to the following equations:

$$s = f_c c b_c \quad \text{---------- (21a)}$$

where s is half the shearing force between the concrete slab and the top steel section.

$$V_c a = \tfrac{1}{2} f_c b_c c^2. \quad \text{---------- (21b)}$$

$$s = f_{sT}(s_T t_w + bt - 2b\bar{y}_T). \quad \text{---------- (21c)}$$

$$V_{sT} a = f_{sT}[s_T t_w(\tfrac{1}{2} s_T + t) + \tfrac{1}{2} b(t^2 - 2\bar{y}_T^2)]. \quad \text{---------- (21d)}$$

$$\bar{y}_B = \frac{A_B}{2b}. \quad \text{---------- (21e)}$$

$$V_{sB} a = f_{sB}[s_B t_w(\tfrac{1}{2} s_B + t) + \tfrac{1}{2} b(t^2 - 2\bar{y}_B^2)]. \quad \text{---------- (21f)}$$

Solving for f_c from equations (17) and (21b),

$$f_c^2[c^2(f'_c + f'_t)^2 + 4a^2(f'_c f'_t)] - f_c[(4a^2 f'_c f'_t(f'_c - f'_t)] - 4a^2(f'_c f'_t)^2 = 0. \quad \text{---------- (22)}$$

Notice also that equilibrium and failure considerations require the point at contraflexure to occur at the midpoint of the hole.

Combining equations (18) and (21d), (21a) and (21c) leads to

$$f_{sT} = \frac{A'_{sT} a f_y}{\sqrt{(A'_{sT} a)^2 + 3[s_T t_w (\frac{1}{2} s_T + t) + \frac{1}{2} b(t^2 - 2 \bar{y}_T^2)]^2}} \quad \text{--- (23)}$$

and

$$\bar{y}_T = \frac{f_{sT}(s_T t_w + bt) - f_c b_c d}{2b f_{sT}} \cdot \quad \text{---------- (24)}$$

$\bar{y}_T$ and f_{sT} in equations (23) and (24) are determined by a trial and error method. Experience with a number of numerical examples has shown convergence to occur fairly rapidly.

From equations (19) and (21f),

$$f_{sB} = \frac{A'_{sB} a f_y}{\sqrt{(A'_{sB} a)^2 + 3[s_B t_w (\frac{1}{2} s_B + t) + \frac{1}{2} b(t^2 - 2 \bar{y}_B^2)]^2}} \cdot \quad \text{-- (25)}$$

Referring to Fig. 12 (NA_T in concrete slab and NA_B in web), and independently considering the equilibrium of forces of the three free body diagrams and their moments about points A and B leads to the following second set of equations:

$$s = f_c b_c (c - 2 \bar{y}_T) \cdot \quad \text{---------- (26a)}$$

$$V_c a = \frac{1}{2} f_c b_c (c^2 - 2 \bar{y}_T^2) \cdot \quad \text{---------- (26b)}$$

$$s = A_{sT} f_{sT} \cdot \quad \text{---------- (26c)}$$

$$V_{sT} a = f_{sT} [\frac{1}{2} bt^2 + s_T t_w (\frac{1}{2} s_T + t)] \cdot \quad \text{---------- (26d)}$$

$$\bar{y}_B = \frac{t_w (s_B + 2t) - bt}{2 t_w} \cdot \quad \text{---------- (26e)}$$

$$V_{sB}{}^{a} = \frac{1}{2} f_{sB}[t_w(s_B + t - \bar{y}_B)(s_B + t + \bar{y}_B)$$

$$- t_w(\bar{y}_B{}^2 - t^2) - bt^2]. \text{ ---------- (26f)}$$

From equations (18) and (26d),

$$f_{sT} = \frac{A'_{sT}af_y}{\sqrt{(A'_{sT}a)^2 + 3[\frac{1}{2}bt^2 + s_Tt_w(\frac{1}{2}s_T + t)]^2}} . \text{ ---------- (27)}$$

Combining equations (17) and (26a), (26b) and (26c) then solving for f_c leads to the quadratic,

$$f_c{}^2\left[1 + \frac{(f'_c + f'_t)^2(c^2 - 2\bar{y}_T{}^2)^2}{4c^2a^2(f'_cf'_t)}\right] - f_c(f'_c - f'_t) - f'_cf'_t = 0. \quad (28)$$

and

$$\bar{y}_T = \frac{f_cb_cc - A_{sT}f_{sT}}{2f_cb_c} . \text{ ---------- (29)}$$

The terms f_c and $\bar{y}_T$ in equations (28) and (29) are determined by trial and error method.

From equations (19) and (26f),

$$f_{sB} = A'_{sB}af_y/\{(A'_{sB}a)^2 + \frac{3}{4}[t_w(s_B + t - \bar{y}_B)(s_B + t + \bar{y}_B)$$

$$- t_w(\bar{y}_B{}^2 - t^2) - bt^2]^2\}^{1/2}. \text{ ---------- (30)}$$

In solving numerical examples the locations of the neutral axes must be determined first and the proper equations used thereafter.

The values of V_u obtained for the three beams using the above equations were 177^K, 117^K and 134^K of which an average of 88% of the total shear was carried by the concrete. Test results of the same beams were much lower (31.4^K, 35.4^K, 12.4^K), but the ratio, $\theta = M_u/V_u$ was very high (7 ft., 9 ft., 33 ft.) for these beams.

Model 1, Case b

In case b, for a given ratio, $\theta = M_u/V_u$ a procedure similar to the one followed in case a to determine V_u was used with the addition of the equation for M_u. Two sets of equations were developed, depending on the location of the neutral axes. The first set is for the case when the top right neutral axis $\bar{y}_{TR}$ was in the steel flange and the bottom right neutral axis $\bar{y}_{BR}$ was in the web. In the second set the top right neutral axis is in the concrete slab and the bottom right neutral axis is in the steel flange.

In Fig. 13, by independantly considering the equilibrium of forces of the three free body diagrams and their moments about points A and B one obtains the following equations:

$$s = f_c b_c (c - \bar{y}_{TL}) \quad \text{---------- (31a)}$$

where $\bar{y}_{TL}$ is the location of the top neutral axis at the left edge (low moment) of the opening.

$$V_c a = \frac{1}{2} f_c b_c (c^2 - \bar{y}_{TL}^2). \quad \text{---------- (31b)}$$

$$s = f_{sT}(A_{sT} - b\bar{y}_{TR}). \quad \text{---------- (31c)}$$

$$2V_{sT} a = f_{sT}[b(t^2 - \bar{y}_{TR}^2) + s_T t_w (2t + s_T)]. \quad \text{---------- (31d)}$$

$$\bar{y}_{BL} b = t_w (s_B + t - \bar{y}_{BR}), \quad \text{---------- (31e)}$$

where $\bar{y}_{BL}$ is the location of the bottom neutral axis at the left edge of the opening.

$$2V_{sB} a = f_{sB}[t_w (s_B + t - \bar{y}_{BR})(s_B + t + \bar{y}_{BR}) - b\bar{y}_{BL}^2] \quad \text{------- (31f)}$$

The equation for the moment at the center of the opening M_u was found by adding up the summation of moments at the left edge $(M_u - M_v)$

about point D, to the summation of moments at the right edge $(M_u + M_v)$ about point B. This leads to the equation

$$2M_u = f_c b_c \bar{y}_{TL}(\bar{y}_{TL} + 2d) + f_{sT} b \bar{y}_{TR}(2d - \bar{y}_{TR}) + f_{sB} t_w (t^2 - \bar{y}_{BR}^2) + f_{sB} b(\bar{y}_{BL}^2 - t^2) \quad \text{---------- (32)}$$

$$\theta = M_u / V_u \quad \text{---------- (33)}$$

in which θ is known.

From equations (17) and (31b),

$$ab_c c\sqrt{f_c' f_t'\left[1 - \left(\frac{2f_c - f_c' + f_t'}{f_c' + f_t'}\right)^2\right]} = f_c b_c (c^2 - \bar{y}_{TL}^2). \quad \text{-------- (34a)}$$

From equations (18) and (31d),

$$2aA_{sT}'\sqrt{\tfrac{1}{3}(f_y^2 - f_{sT}^2)} = f_{sT}[b(t^2 - \bar{y}_{TR}^2) + s_T t_w(2t + s_T)]. \quad \text{--- (34b)}$$

From equation (19) and (31f),

$$2aA_{sB}'\sqrt{\tfrac{1}{3}(f_y^2 - f_{sB}^2)} = f_{sB}[t_w(s_B + t - \bar{y}_{BR})(s_B + t + \bar{y}_{BR}) - b\bar{y}_{BL}^2]. \quad \text{---------- (34c)}$$

Eliminating M_u by combining equations (32) and (33) then substituting for V_u,

$$2\theta\{\frac{cb_c}{2}\sqrt{f_c' f_t'\left[1 - \left(\frac{2f_c - f_c' + f_t'}{f_c' + f_t'}\right)^2\right]} + A_{sT}'\sqrt{\tfrac{1}{3}(f_y^2 - f_{sT}^2)} + A_{sB}'\sqrt{\tfrac{1}{3}(f_y^2 - f_{sB}^2)}\} = f_c b_c \bar{y}_{TL}(\bar{y}_{TL} + 2d) + f_{sT} b \bar{y}_{TR}(2d - \bar{y}_{TR}) + s_B t_w(t^2 - \bar{y}_{BR}^2) + f_{sB} b(\bar{y}_{BL}^2 - t^2)$$

Eliminating the square root terms by using equations (34) then simplifying leads to,

$$f_c b_c[\bar{y}_{TL}^2(1 + \frac{\theta}{a}) + 2d\,\bar{y}_{TL} - \frac{\theta}{a}c^2]$$

$$+ f_{sT} b[\bar{y}_{TR}^2(\frac{\theta}{a} - 1) + 2d\,\bar{y}_{TR} - \frac{\theta}{a}t^2 - \frac{\theta}{ab}t_w s_T(2t + s_T)]$$

$$+ f_{sB} t_w[\bar{y}_{BR}^2(\frac{\theta}{a} - 1) + \frac{\theta}{a}\frac{b}{t_w}\bar{y}_{BL}^2 + t^2 - \frac{\alpha}{a}(s_B + t)^2] = 0. \quad (35)$$

Equating the summation of horizontal forces at the left edge to zero,

$$f_c b_c \bar{y}_{TL} + f_{sT}\, b\bar{y}_{TR} - f_{sB}(A_{sB} - 2\bar{y}_{BL}b) = 0. \text{----------} \quad (36)$$

Combining equations (31a) and (31c) then rearranging

$$f_c b_c \bar{y}_{TL} - f_{sT}\, b\bar{y}_{TR} = f_c b_c c - f_{sT} A_{sT}, \text{----------} \quad (a)$$

Rearranging equations (31e) and (36),

$$b\bar{y}_{BL} + t_w \bar{y}_{BR} = t_w(s_B + t), \text{----------} \quad (b)$$

$$f_c b_c \bar{y}_{TL} + f_{sT}\, b\bar{y}_{TR} + 2f_{sB} b\bar{y}_{BL} = f_{sB} A_{sB}. \text{----------} \quad (c)$$

Adding equations (c) and (a),

$$\bar{y}_{TL} = \frac{1}{2f_c b_c}(f_c b_c c - f_{sT} A_{sT} + f_{sB} A_{sB} - 2f_{sB} b\bar{y}_{BL}), \text{------} \quad (37a)$$

Subtracting Eq. (a) from Eq. (c),

$$\bar{y}_{TR} = \frac{1}{2f_{sT} b}(f_{sB} A_{sB} - f_c b_c c + f_{sT} A_{sT} - 2f_{sB} b\bar{y}_{BL}), \text{------} \quad (37b)$$

From Eq. (b)

$$\bar{y}_{BR} = s_B + t - \frac{b}{t_w}\bar{y}_{BL} \text{----------} \quad (37c)$$

Solving for $\bar{y}_{BL}$ using equations (37a), (37b), (37c) and (36) leads to the quadratic,

$$\bar{y}_{BL}^2\left[\frac{f_{sB}^2 b^2}{f_c b_c}\left(1+\frac{\theta}{a}\right)+\frac{f_{sB}^2 b}{f_{sT}}\left(\frac{\theta}{a}-1\right)+\frac{f_{sB}b^2}{t_w}\left(\frac{\theta}{a}-1\right)\right.$$

$$\left.+\frac{f_{sB}\theta b}{a}\right]-\bar{y}_{BL}\left[\frac{R_1 f_{sB} b}{f_c b_c}\left(1+\frac{\theta}{a}\right)+4f_{sB}bd+\frac{R_2 f_{sB}}{f_{sT}}\left(\frac{\theta}{a}-1\right)\right.$$

$$\left.+2f_{sB}(s_B+t)\left(\frac{\theta}{a}-1\right)\right]+\left[\frac{R_1^2}{4f_c b_c}\left(1+\frac{\theta}{a}\right)+2R_1 d-Z_1 f_c b_c\right.$$

$$\left.+\frac{R_2^2}{4f_{sT}b}\left(\frac{\theta}{a}-1\right)-Z_2 f_{sT} b+f_{sB}t_w\left(\frac{\theta}{a}-1\right)(s_B+t)^2\right.$$

$$\left.+Z_3 f_{sB} t_w\right]=0 \qquad (38)$$

in which

$$R_1 = f_c b_c - f_{sT}A_{sT} + f_{sB}A_{sB};$$

$$R_2 = f_{sB}A_{sB} - f_c b_c c + f_{sT}A_{sT};$$

$$Z_1 = \frac{\theta}{a}c^2;$$

$$Z_2 = \frac{\theta}{a}t^2 + \frac{\theta}{ab}t_w s_T(2t+s_T);$$

$$Z_3 = t^2 - \frac{\theta}{a}(s_B+t)^2.$$

The values of f_c, f_{sT}, f_{sB}, $\bar{y}_{TL}$, $\bar{y}_{TR}$, $\bar{y}_{BL}$ and $\bar{y}_{BR}$ can probably be determined by a trial and error procedure. $\bar{y}_{BL}$, $\bar{y}_{BR}$, $\bar{y}_{TL}$ and $\bar{y}_{TR}$ can be determined from equations (38) and (37) by assuming reasonable values for f_c, f_{sT}, and f_{sB}. The values of f_c, f_{sT}, and f_{sB} are then computed from equations (34a), (34b) and (34c). This iteration process is repeated until there is a convergence.

Referring to Fig. 14 ($\bar{y}_{TR}$ in concrete slab and $\bar{y}_{BR}$ in steel flange) and independantly considering the equilibrium of forces of the three

free body diagrams and their moments about points A and B lead to the following second set of equations.

$$s = f_c b_c (c - \bar{y}_{TL} - \bar{y}_{TR}). \text{---------- (39a)}$$

$$2aV_c = f_c b_c [(c^2 - \bar{y}_{TL}^2) - \bar{y}_{TR}^2]. \text{---------- (39b)}$$

$$s = f_{sT} A_{sT}. \text{---------- (39c)}$$

$$2aV_{sT} = f_{sT}[bt^2 + s_T t_w (s_T + 2t)]. \text{---------- (39d)}$$

$$s_B t_w + b(t - \bar{y}_{BR}) = b\bar{y}_{BL}. \text{---------- (39e)}$$

$$2aV_{sB} = f_{sB}[s_B t_w (s_B + 2t) + b(t^2 - \bar{y}_{BR}^2 - \bar{y}_{BL}^2)]. \text{---------- (39f)}$$

The equation for the moment at the centerline of the opening M_u is obtained in a similar manner as equation (32).

$$2M_u = f_c b_c (\bar{y}_{TL} - \bar{y}_{TR})(\bar{y}_{TL} + \bar{y}_{TR} + 2d)$$

$$- f_{sB} b(\bar{y}_{BR}^2 - \bar{y}_{BL}^2). \text{---------- (40)}$$

From equations (17) and (39b),

$$acb_c \sqrt{f_c' f_t' \left[1 - \left(\frac{2f_c - f_c' + f_t'}{f_c' + f_t'}\right)^2\right]} = f_c b_c [(c^2 - \bar{y}_{TL}^2)$$

$$- \bar{y}_{TR}^2]. \text{---------- (41a)}$$

From equations (18) and (39d),

$$2aA_{sT}' \sqrt{\tfrac{1}{3}(f_y^2 - f_{sT}^2)} = f_{sT}[bt^2 + s_T t_w (s_T + 2t)]. \text{---------- (41b)}$$

From equations (19) and (39f),

$$2aA_{sB}' \sqrt{\tfrac{1}{3}(f_y^2 - f_{sB}^2)} = f_{sB}[s_B t_w (s_B + 2t) + b(t^2 - \bar{y}_{BR}^2$$

$$- \bar{y}_{BL}^2)]. \text{---------- (41c)}$$

From equation (41b),

$$f_{sT} = \frac{2aA'_{sT}f_y}{\sqrt{(2aA'_{sT})^2 + 3[bt^2 + s_T t_w(s_T + 2t)]^2}} \cdot \text{---------- (42)}$$

Eliminating M_u by combining equations (33) and (40) then substituting for V_u,

$$2\theta\left\{\frac{cb_c}{2}\sqrt{f'_c f'_t\left[1 - \left(\frac{2f_c - f'_c + f'_t}{f'_c + f'_t}\right)^2\right]} + V_{sT} + A'_{sB}\sqrt{\frac{1}{3}(f_y^2 - f_{sB}^2)}\right\}$$

$$= f_c b_c(\bar{y}_{TL} - \bar{y}_{TR})(\bar{y}_{TL} + \bar{y}_{TR} + 2d) - f_{sB}b(\bar{y}_{BR}^2 - \bar{y}_{BL}^2).$$

Eliminating the square root terms by using equations (41), then simplifying,

$$f_c b_c[\bar{y}_{TR}^2(1 - \tfrac{\theta}{a}) - \bar{y}_{TL}^2(1 + \tfrac{\theta}{a}) + 2d(\bar{y}_{TR} - \bar{y}_{TL})]$$

$$+ \frac{\theta}{a}(f_c b_c c^2 + V_{sT}) + f_{sB}b[\bar{y}_{BR}^2(1 - \tfrac{\theta}{a}) - \bar{y}_{BL}^2(1 + \tfrac{\theta}{a})]$$

$$+ \frac{f_{sB}b\theta}{a}[\tfrac{1}{b}s_B t(s_B + 2t) + t^2] = 0. \text{---------- (43)}$$

The value of V_{sT} in equation (43) can be computed directly from equations (42) and (18).

Equating the summation of horizontal forces at the right edge to zero (the stress distribution shown at the right edge in Fig. 12 is valid),

$$f_c b_c(c - 2\bar{y}_{TR}) - A_{sT}f_{sT} + f_{sB}(A_{sB} - 2b\bar{y}_{BR}) = 0. \text{--------- (44)}$$

Rearranging equation (44),

$$2f_c b_c \bar{y}_{TR} + 2f_{sB}b\bar{y}_{BR} = f_c b_c c - f_{sT}A_{sT} + f_{sB}A_{sB}. \text{---------- (d)}$$

From equations (39a) and (39c),

$$2f_c b_c \bar{y}_{TR} + 2f_c b_c \bar{y}_{TL} = 2f_c b_c c - 2f_{sT}A_{sT}. \text{---------- (e)}$$

From equation (39e),

$$b\bar{y}_{BR} + b\bar{y}_{BL} = A_{sB}. \text{---------- (f)}$$

From equation (f),

$$\bar{y}_{BL} = \frac{1}{b} A_{sB} - \bar{y}_{BR}. \text{---------- (45a)}$$

Subtracting Eq. (d) from Eq. (e),

$$\bar{y}_{TL} = \frac{1}{2f_c b_c} (f_c b_c c - f_{sT} A_{sT} - f_{sB} A_{sB} + 2f_{sB} b\bar{y}_{BR}). \text{------ (45b)}$$

From equation (d)

$$\bar{y}_{TR} = \frac{1}{2f_c b_c} (f_c b_c c - f_{sT} A_{sT} + f_{sB} A_{sB} - 2f_{sB} b\bar{y}_{BR}). \text{------ (45c)}$$

Solving for $\bar{y}_{BR}$ using equations (45) and (43) leads to the quadratic,

$$\bar{y}_{BR}^2 [f_{sB} b(1 - \frac{\theta}{a}) - \frac{2\theta f_{sB}^2 b^2}{a f_c b_c} - (1 + \frac{\theta}{a})]$$

$$- \bar{y}_{BR} \left\{ \frac{f_{sB} b}{f_c b_c} [R_4(1 - \frac{\theta}{a}) + R_3(1 + \frac{\theta}{a})] \right.$$

$$\left. + 2f_{sB}[2bd + A_{sB}(1 + \frac{\theta}{a})] \right\}$$

$$+ \frac{1}{4f_c b_c} [R_4^2(1 - \frac{\theta}{a}) - R_3^2(1 + \frac{\theta}{a})] + d(R_4 - R_3)$$

$$- \frac{A_{sB}^2 f_{sB}}{b} (1 + \frac{\theta}{a}) + Z_4 = 0. \text{---------- (46)}$$

in which

$$R_3 = f_c b_c c - f_{sT} A_{sT} - f_{sB} A_{sB};$$

$$R_4 = f_c b_c c - f_{sT} A_{sT} + f_{sB} A_{sB};$$

$$Z_4 = \frac{\theta}{a} \{f_c b_c c^2 + V_{sT} + f_{sB} b[\frac{s_B t}{b}(s_B + 2t) + t^2]\}.$$

In case b if the following combinations of the locations of the neutral axes should occur, $\bar{y}_{TR}$ in concrete slab and $\bar{y}_{BR}$ in web or $\bar{y}_{TR}$ in steel flange and $\bar{y}_{BR}$ in steel flange, then equations (32) thru (38) and equations (40) thru (46) will change. The new equations can be developed following a procedure similar to the one used in obtaining equations (32-38) or equations (40-46).

Model 2, Case a

In this model the tensile stress of the concrete f_c which was assumed to be equal to the compressional stress f_c in the first model is set equal to γf_c, where γ is some reduction factor. The effect this reduction will have on the shearing force V_c the concrete carries, and the compressive stress f_c were studied by allowing them both to change. Equilibrium considerations of the steel section (see Fig. 12) will require the point of contraflexure to occur at the midpoint of the opening. This means the point of contraflexure for the concrete section will have to occur at its midpoint for there can only be one point of contraflexure.

Two sets of equations were developed for the free body diagram of the concrete block for the two states of stress defined below.

State 1: State 1 is similar to Model 1 (see Fig. 15) where,

$$f_{c_1} = f_c(1 - \varepsilon) = f_c, \text{ i.e. } \varepsilon = 0;$$

$$f_{t_1} = \gamma f_{c_1} = (1 - \delta) f_c = f_c, \text{ i.e. } \delta = 0;$$

$$V_{c_1} = V_c.$$

Also for this state as in Model 1, $\bar{y}_{TL_1} = \bar{y}_{TR_1} = \bar{y}_T$.

State 2: $f_{c_2} = f_c(1 - \varepsilon)$, i.e. $\varepsilon \neq 0$ or 1;

$$f_{t_2} = \gamma f_{c_2} = (1 - \delta) f_{c_2}, \text{ i.e. } \delta \neq 0.$$

Figures 15 and 16 show the two states for the concrete slab and are referred to in the derivation of the following equations. The stress distribution in the steel is as shown in Fig. 12. In Figs. 15 and 16, consideration of the equilibrium of forces of the right and left free body diagrams then their moments about points A and B leads to the following equations:

$$s = f_c b_c (c - 2\bar{y}_T). \text{ ---------- (47a)}$$

$$V_c a = \frac{1}{2} f_c b_c (c^2 - 2\bar{y}_T^2). \text{ ---------- (47b)}$$

$$s = (1 - \varepsilon) f_c b_c [c - \bar{y}_{TR_2}(2 - \delta)]. \text{ ---------- (48a)}$$

$$V_{c_2} a = \frac{1}{2}(1 - \varepsilon) f_c b_c [c^2 - \bar{y}_{TR_2}^2 (2 - \delta)]. \text{ ---------- (48b)}$$

$$s = (1 - \varepsilon) f_c b_c [(1 - \delta)c - \bar{y}_{TL_2}(2 - \delta)]. \text{ ---------- (48c)}$$

$$V_{c_2} a = \frac{1}{2}(1 - \varepsilon) f_c b_c [(1 - \delta)c^2 - \bar{y}_{TL_2}^2 (2 - \delta)]. \text{ ---------- (48d)}$$

Equations (47a) and (47b) refer to both the right and left free body diagrams of Fig. 15, Eqs. (48a) and (48b) refer to the right free body diagram of Fig. 16 and Eqs. (48c) and (48d) refer to the left free body diagram of Fig. 16.

From equations (47a) and (48a),

$$\bar{y}_{TR_2} = \frac{2\bar{y}_T - \varepsilon c}{(2 - \delta)(1 - \varepsilon)}. \text{ ---------- (49a)}$$

From equations (47a) and (48c),

$$\bar{y}_{TL_2} = \frac{c[(1 - \varepsilon)(1 - \delta) - 1] + 2\bar{y}_T}{(2 - \delta)(1 - \varepsilon)}. \text{ ---------- (49b)}$$

From equations (47b) and (48b),

$$\bar{y}_{TR_2}^2 = \frac{c^2(1 - \varepsilon) - \beta(c^2 - 2\bar{y}_T^2)}{(2 - \delta)(1 - \varepsilon)} \text{ ---------- (50a)}$$

in which $\beta = V_{c_2}/V_c$.

From equations (47b) and (48d),

$$\bar{y}_{TL_2}^2 = \frac{(1 - \delta)(1 - \varepsilon)c^2 - \beta(c^2 - 2\bar{y}_T^2)}{(1 - \varepsilon)(2 - \delta)} \text{ ---------- (50b)}$$

Solving for β from Eqs. (49a) and (50a),

$$\beta = \frac{1}{c^2 - 2\bar{y}_T^2}\left[c^2(1 - \varepsilon) - \frac{(2\bar{y}_T - \varepsilon c)^2}{(2 - \delta)(1 - \varepsilon)}\right] \text{ ---------- (51a)}$$

Solving for β from Eqs. (49b) and (50b),

$$\beta = \frac{1}{c^2 - 2\bar{y}_T^2}\left\{c^2(1 - \delta)(1 - \varepsilon) - \frac{([(1 - \varepsilon)(1 - \delta) - 1]\, c + 2\bar{y}_T)^2}{(1 - \varepsilon)(2 - \delta)}\right\} \text{ ---------- (51b)}$$

Equating Eq. (51a) to Eq. (51b) and solving for ε leads to,

$$\delta[\varepsilon(2\bar{y}_T - c) + c - 2\bar{y}_T] = 0. \text{ ---------- (52)}$$

Examining equation (52) shows that either $\delta = 0$, meaning $f_t = f_c$ or $\varepsilon = 1$, meaning $f_c = 0$ which is impossible. This leads to the conclusion that in order for statics to be satisfied for Model 2 as it stands, then f_t must be equal to f_c. In reality the tensile stress of concrete at failure is much less than its compressive stress and therefore the second model should be changed accordingly to reflect this.

CONCLUSIONS

An elastic analysis of steel-concrete composite beams with web openings has been made based on Vierendeel's method. A method of solution and a short computer program to facilitate the process have been presented. The results obtained using the method presented here showed a reasonable agreement with results obtained from a finite element computer program. This justified the suitability of the Vierendeel approach to the problem. Of further interest is the fact that a fairly high percent of the total shear is carried by the concrete, especially when uncracked. A general method of approach to the ultimate strength analysis based on the findings in the elastic analysis was also developed and discussed.

RECOMMENDATIONS FOR FURTHER RESEARCH

The author recommends further research in the development of equations for the second and third models for ultimate strength analysis. Experience from the first model shows that the equations will be lengthy, and a trial and error method would be necessary to solve them. A computer program similar to the one developed for the elastic analysis would very likely be required to facilitate the iteration process.

ACKNOWLEDGMENTS

The author first of all wishes to express his sincere gratitude to his major professor, Dr. S. E. Swartz, for his excellent teaching and advice. Appreciation is also extended to Dr. P. B. Cooper and Dr. H. S. Walker for serving as committee members. Finally, sincere thanks is extended to the National Science Foundation (Grant No. ENG 76-19045) and the Engineering Experiment Station of Kansas State University for supporting this research.

APPENDIX I - REFERENCES

1. Knostman, Harry D., Cooper, Peter B., and Snell, Robert R., "Shear Force Distribution at Eccentric Web Openings," Journal of the Structural Division, ASCE, Vol. 103, No. ST6, June 1977.

2. Tasuji, Ebrahim M., Slate, Floyd O. and Nilson, Arthur H., "Stress-Strain Response and Fracture of Concrete in Biaxial Loading," ACI Journal, Vol. 75, No. 7, July 1978.

3. Taylor, M. A., Romstad, K. M., Herrmann, L. R., and Henry, M. R., "A Finite Element Computer Program for the Prediction of the Behavior of Reinforced and Prestressed Concrete Structures Subject to Cracking," University of California at Davis, No. N62399-70-C-0023, June 1972.

APPENDIX II - NOTATION

A - Net cross-section area

A_B - Bottom steel area

A_T - Top composite area

A_{Ts} - Top steel area

a - One-half length of opening

b - Steel flange width

b_c - width of concrete slab

b_s - Width of transformed concrete slab

c - Thickness of concrete slab

c_r - Thickness of cracked concrete slab

d - Steel section depth

E - Modulus of elasticity for steel

e - Opening eccentricity

f_c - Normal compressive stress in concrete

f'_c - Compressive strength of concrete

f_{sB} - Normal stress in bottom steel section

f_{sT} - Normal stress in top steel section

f'_t - Tensile strength of concrete

f_{Vc} - Shearing stress in concrete

f_y - Yield stress of steel

f_b^b - Elastic steel stress at bottom of bottom section

f_b^t - Elastic steel stress at top of bottom section

f_c^b - Elastic concrete stress at bottom of slab

f_c^t - Elastic concrete stress at top of slab

f_t^b - Elastic steel stress at bottom of top section

f_t^t - Elastic steel stress at top of top steel section

G - Modulus of rigidity for steel

h - Opening depth

I_B - Bottom section moment of inertia

I_N - Moment of inertia of net composite section

I_T - Top composite section moment of inertia

I_{Ts} - Top steel moment of inertia

K_B - Shearing deflection coefficient of bottom section

K_T - Shearing deflection coefficient of top composite section

K_{Ts} - Shearing deflection coefficient of top steel section

$M_B = V_B x$

M_p - Moment at center of opening

$M_T = V_T x$

M_u - Moment at center of opening at failure

n - Modular ratio

P - Load

s - Half the shearing force between concrete slab and top steel flange

s_B - Depth of web section in bottom tee at opening

s_T - Depth of web section in top tee at opening

$\bar{s}$ - Distance from top of top steel section to NA_{TS}

t - Steel flange thickness

t_w - Steel web thickness

V - Total shear applied to beam at opening

V_B - Shear carried by bottom section

V_c - Shear carried by concrete section

V_T - Shear carried by top composite section

V_u - Total shear at failure carried by section

x - Distance from center of opening to desired location ($-a \leq x \leq a$)

y_B - Distance from NA_B to depth desired in bottom section

$\bar{y}_B$ - Distance from bottom of bottom tee section to NA_B

y_N - Distance from NA(net) to depth desired

$\bar{y}_N$ - Distance from top of concrete slab to NA(net)

y_T - Distance from NA_T to depth desired in top section

$\bar{y}_T$ - Distance from top of concrete slab to NA_T

$\alpha = V_T/V$

$\beta = V_{c_2}/V_c$

$\beta' = V_T/V_B$

$\theta = M_u/V_u$

APPENDIX III - SHEAR DEFLECTION COEFFICIENTS

Three principal shear deflection coefficients are required for the purpose of computing the total shearing force distribution, to the top (composite) and bottom sections, and also for the top steel section for the case when all concrete is assumed cracked. These are K_T, K_B and K_{Ts}. To determine these the strain energy approach is used and also the shearing stresses τ and strains γ are assumed linearly proportional. For a given small volume v, the shearing strain energy is

$$u = \frac{\tau^2}{2G} \qquad \text{(53a)}$$

where

$$\tau = VQ/It.$$

For a given length s, the total shearing strain energy U can be written as

$$U = \int_0^s dx \int_A \frac{V^2Q^2}{2I^2t^2G} dA \qquad \text{(53b)}$$

in which Q is the first moment of the cross-sectional area, I the centroidal moment of inertia and t the thickness. Rewriting the shearing strain energy equation

$$U = \int_0^s \frac{V^2}{2AG} dx \left[\frac{A}{I_2} \int_A \frac{Q^2}{t^2} dA\right]. \qquad \text{(53c)}$$

The term in the bracket is dimensionless and depends only on the cross-sectional area. This constant is referred to as the shear deflection coefficient K. Hence,

$$K = \frac{A}{I^2} \int_A \frac{Q^2}{t^2} dA. \qquad \text{(53d)}$$

Referring to Fig. 4a, K_T is evaluated by separating the integration of the cross-section into three parts: the concrete slab, the flange and the web.

$$K_T = \frac{A_T}{I_T^2} (K_1 + K_2 + K_3). \text{---------- (54)}$$

$$K_1 = \frac{1}{b_s^2} \int_A Q^2 \, dA;$$

in which

$$Q^2 = \left(\int_y^{Q_1} b_s y dy\right)^2$$

$$= \frac{b_s^2}{4} (Q_1^4 - 2Q_1^2 y^2 + y^4).$$

Therefore,

$$K_1 = \frac{b_s}{4} \int_{-Q_2}^{Q_1} (Q_1^4 - 2Q_1^2 y^2 + Q^4) \, dy.$$

$$K_1 = \frac{b_s}{4} \left[Q_1^4 (Q_1 + Q_2) - \frac{2}{3} Q_1^2 (Q_1^3 + Q_2^3)\right.$$

$$\left. + \frac{1}{5}(Q_1^5 + Q_2^5)\right]. \text{---------- (55a)}$$

Similarly,

$$K_2 = \frac{1}{b^2} \int_A Q^2 dA,$$

in which

$$Q^2 = \left[\int_y^{Q_4} b y d_y + \frac{1}{2} (Q_4 + Q_5) s_T t_w\right]^2$$

$$= \left[\frac{b}{2} (Q_4^2 - y^2) + \frac{1}{2} (Q_4 + Q_5) s_T t_w\right]^2.$$

Therefore,

$$K_2 = \frac{1}{b^2} \int_{Q_3}^{Q_4} [\frac{b}{2}(Q_4^2 - y^2) + \frac{1}{2}(Q_4 + Q_5)\, s_T t_w]^2\, dy.$$

$$K_2 = \frac{b}{4} [Q_4^4(Q_4 - Q_3) - \frac{2}{3} Q_4^2 (Q_4^3 - Q_3^3) + \frac{1}{5}(Q_4^5 - Q_3^5)]$$

$$+ \frac{1}{2}(Q_4 + Q_5)\, s_T t_w [Q_4^2 (Q_4 - Q_3) - \frac{1}{3}(Q_4^3 - Q_3^3)]$$

$$+ \frac{1}{b} [\frac{1}{2}(Q_4 + Q_5)\, s_T t_w]^2 (Q_4 - Q_3). \text{---------- (55b)}$$

Similarly,

$$K_3 = \frac{1}{t_w^2} \int_A Q^2 dA,$$

in which

$$Q^2 = (\int_y^{Q_5} t_w y\, dy)^2$$

$$= \frac{t_w^2}{4} (Q_5^2 - y^2)^2.$$

Therefore,

$$K_3 = \frac{t_w}{4} \int_{Q_4}^{Q_5} (Q_5^4 - 2Q_5^2 y^2 + y^4)\, dy.$$

$$K_3 = \frac{t_w}{4} [Q_5^4 (Q_5 - Q_4) - \frac{2}{3} Q_5^2 (Q_5^3 - Q_4^3)$$

$$+ \frac{1}{5}(Q_5^5 - Q_4^5)]. \text{---------- (55c)}$$

Referring to Fig. 4b, K_B is evaluated by separating the integration of the cross-section into two parts, the web and the flange sections.

$$K_B = \frac{A_B}{I_B^2}(K_4 + K_5). \text{---------- (56)}$$

$$K_4 = \frac{1}{t_w^2} \int_A Q^2\, dA,$$

in which

$$Q^2 = (\int_y^{Q_6} t_w y \, dy)^2,$$

$$= \frac{t_w^2}{4} (Q_6^4 - 2Q_6^2 y^2 + y^4).$$

Therefore,

$$K_4 = \frac{t_w}{4} \int_{-Q_7}^{Q_6} (Q_6^4 - 2Q_6^2 y^2 + y^4) \, dy.$$

$$K_4 = \frac{t_w}{4} [Q_6^4 (Q_6 + Q_7) - \frac{2}{3} Q_6^2 (Q_6^3 + Q_7^3) + \frac{1}{5} (Q_6^5 + Q_7^5)]. \quad (57a)$$

Similarly,

$$K_5 = \frac{1}{b^2} \int_A Q^2 \, dA,$$

in which

$$Q^2 = (\int_y^{Q_8} by \, dy)^2$$

$$= \frac{b^2}{4} (Q_8^4 - 2Q_8^2 y^2 + y^4).$$

Therefore,

$$K_5 = \frac{b}{4} \int_{Q_7}^{Q_8} (Q_8^4 - 2Q_8^2 y^2 + y^4) \, dy.$$

$$K_5 = \frac{b}{4} [Q_8^4 (Q_8 - Q_7) - \frac{2}{3} Q_8^2 (Q_8^3 - Q_7^3) + \frac{1}{5} (Q_8^5 - Q_7^5)]. \quad (57b)$$

When all the concrete is assumed cracked, a new value of the top shearing deflection coefficient has to be determined, for it is also assumed that when this occurs, the beam behaves as if the concrete slab were not present.

Hence, referring to Fig. 4c, the shearing deflection coefficient of the top steel section is evaluated by separating the integration of the cross-section into two parts; the flange and the web.

$$K_{Ts} = \frac{A_{Ts}}{I_{Ts}^2} (K_6 + K_7). \text{---------- (58)}$$

$$K_6 = \frac{1}{b^2} \int_A Q^2 dA,$$

in which

$$Q^2 = \left(\int_y^{Q_9} by\, dy\right)^2,$$

$$= \frac{b^2}{4} (Q_9^4 - 2Q_9^2 y^2 + y^4),$$

Therefore,

$$K_6 = \frac{b}{4} \int_{Q_{10}}^{Q_9} (Q_9^4 - 2Q_9^2 y^2 + y^4)\, dy.$$

$$K_6 = \frac{b}{4} \left[Q_9^4 (Q_9 - Q_{10}) - \frac{2}{3} Q_9^2 (Q_9^3 - Q_{10}^3)\right.$$

$$\left. + \frac{1}{5} (Q_9^5 - Q_{10}^5)\right]. \text{---------- (59a)}$$

Similarly,

$$K_7 = \frac{1}{t_w^2} \int_A Q^2 dA,$$

in which

$$Q^2 = \left(\int_y^{Q_{11}} t_w\, y\, dy\right)^2,$$

$$= \frac{t_w^2}{4} (Q_{11}^4 - 2Q_{11}^2 y^2 + y^4).$$

Therefore,

$$K_7 = \frac{t_w}{4} \int_{-Q_{10}}^{Q_{11}} (Q_{11}^4 - 2Q_{11}\, y^2 + y^4)\, dy.$$

$$K_7 = \frac{t_w}{4} [Q_{11}^4 (Q_{11} + Q_{10}) - \frac{2}{3} Q_{11}^2 (Q_{11}^3 + Q_{10}^3)$$

$$+ \frac{1}{5} (Q_{11}^5 + Q_{10}^5). \text{---------- (59b)}$$

APPENDIX IV - SERVICE STRESS EQUATIONS

Referring to Fig. 3 , the service stress equations for the locations indicated are the following:

Concrete Stress at Top of Slab

$$f_c^t = -\frac{M_p \bar{y}_N}{n I_N} - \frac{M_T \bar{y}_T}{n I_T}. \quad \text{(60a)}$$

Concrete Stress at Bottom of Slab (if not cracked)

$$f_c^b = -\frac{M_p (\bar{y}_N - c)}{n I_N} + \frac{M_T (c - \bar{y}_T)}{n I_T}. \quad \text{(60b)}$$

Steel Stress at Top of Top Steel Section

$$f_t^t = n f_c^b. \quad \text{(60c)}$$

Steel Stress at Bottom of Top Section

$$f_c^b = +\frac{M_p (s_T + t + c - \bar{y}_N)}{I_N} + \frac{M_T (s_T + t + c - \bar{y}_T)}{I_T}. \quad \text{(60d)}$$

Steel Stress at Top of Bottom Section

$$f_b^t = \frac{M_p (d + c - s_B - t - \bar{y}_N)}{I_N} - \frac{M_B (s_B + t - \bar{y}_B)}{I_B}. \quad \text{(60e)}$$

Steel Stress at Bottom of Bottom Section

$$f_b^b = \frac{M_p (d + c - \bar{y}_N)}{I_N} + \frac{M_B \bar{y}_B}{I_B}. \quad \text{(60f)}$$

Referring to Fig. 3 for the case $C_r = 0$, the service stress equations for the indicated locations may be written as follows:

Steel Stresses for Top and Bottom of Top Steel Section

$$f_t^t = -\frac{M_p \bar{y}_N}{I_N} - \frac{M_T \bar{y}_T}{I_T}. \quad \text{(61a)}$$

$$f_t^b = -\frac{M_p(\bar{y}_N - t - s_T)}{I_N} + \frac{M_T(s_T + t - \bar{y}_T)}{I_T}. \quad \text{(61b)}$$

Steel Stresses for Top and Bottom of Bottom Section

$$f_b^t = \frac{M_p(d - t - s_B - \bar{y}_N)}{I_N} - \frac{M_B(s_B + t - \bar{y}_B)}{I_B}. \quad \text{(61c)}$$

$$f_b^b = \frac{M_p(d - \bar{y}_N)}{I_N} + \frac{M_B\bar{y}_B}{I_B}, \quad \text{(61d)}$$

where the cross-section properties $\bar{y}_T$, $\bar{y}_N$ and I_N for this case are:

$$\bar{y}_T = \bar{s}, \quad \text{(62a)}$$

$$\bar{y}_N = [A_B(d - \bar{y}_B) + A_{Ts}\,\bar{y}_T]/(A_B + A_{Ts}), \quad \text{(62b)}$$

$$I_N = I_{Ts} + A_{Ts}\,(\bar{y}_N - \bar{y}_T)^2 + I_B + A_B(d - \bar{y}_N - \bar{y}_B)^2. \quad \text{(62c)}$$

Since the stresses are assumed to vary linearly, the top and bottom horizontal forces are easily obtained by multiplying the stresses with the area over which they act.

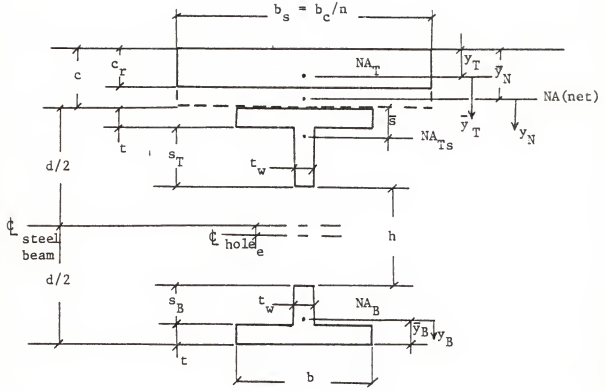

Fig. 1 - Transformed Composite Section at Opening

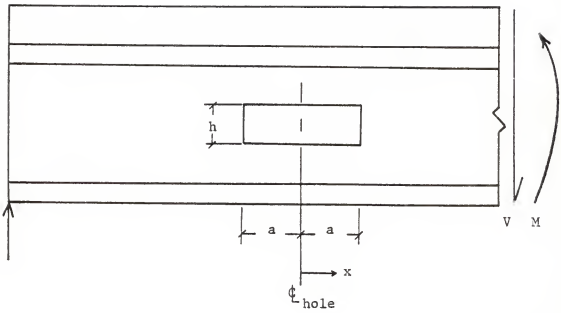

Fig. 2 - Elevation of a Steel-Concrete Composite Beam With Web Opening

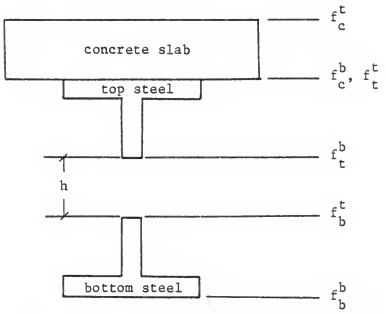

Fig. 3 - Cross Section Locations for Computed Stresses

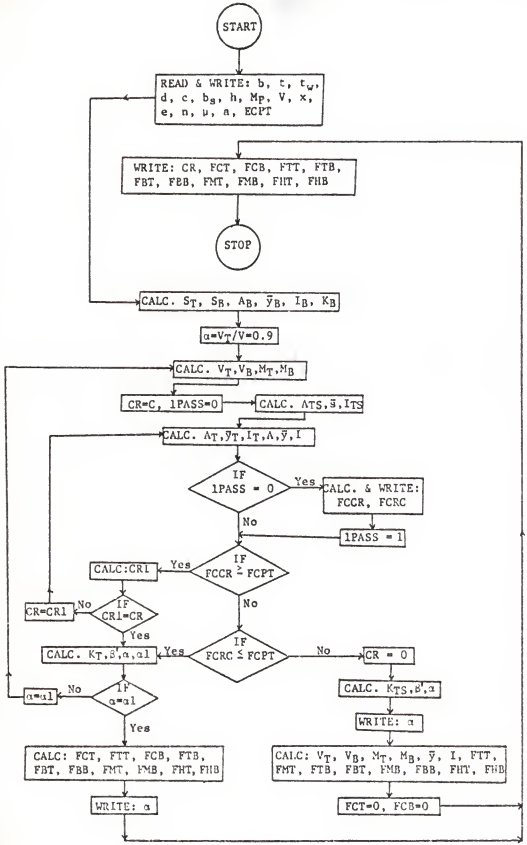

Fig. 3a - Flow Diagram

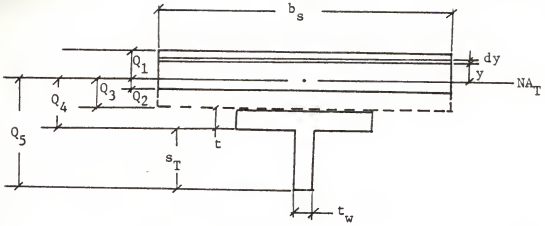

(a) Top Composite Section

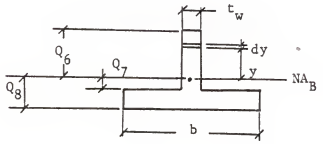

(b) Bottom Steel Section

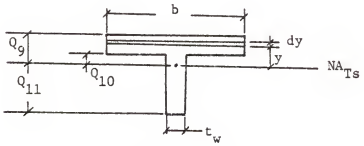

(c) Top Steel Section

Fig. 4 - Geometry Parameters Used in the Calculation of the Shear-Deflection Coefficient

Beam No. 1

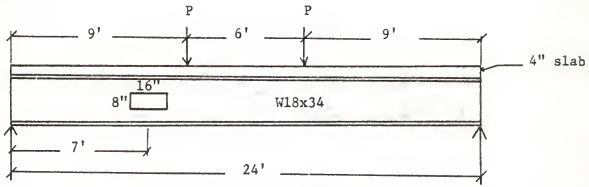

Beam No. 2

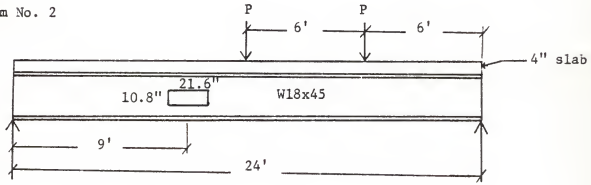

Beam No. 3

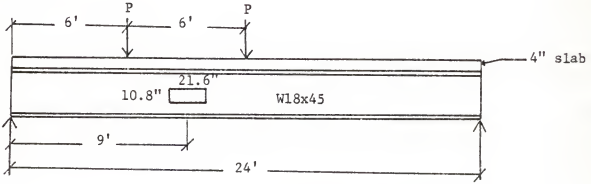

Fig. 5 - Beams Used in Analysis Examples
1 in. = 0.0254 m, 1 ft. = 0.305 m

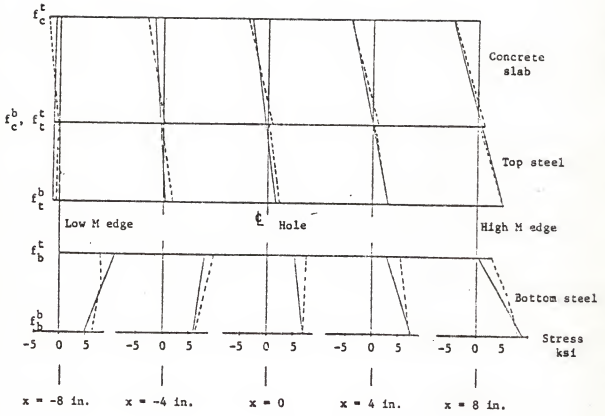

——— Stresses calculated by method of this report

- - - - - - - Stresses obtained from finite element program (3) concrete stresses times ten

Fig. 6 - Longitudinal Stresses in Region of Hole - Beam No. 1
1 in. = 25.4 mm, 1 ksi. = 6.8976 MPa

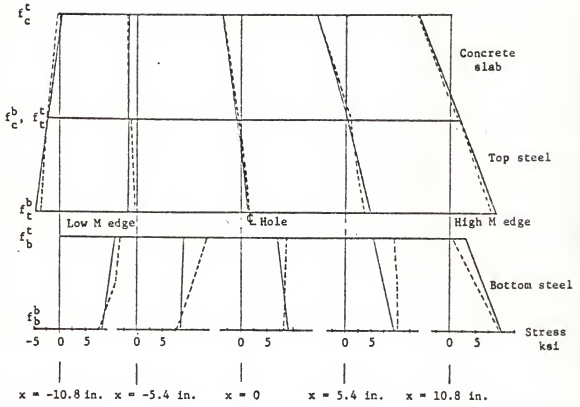

——— Stresses calculated by method of this report

- - - - - - Stresses obtained from finite element program (3) concrete stresses times ten

Fig. 7 - Longitudinal Stresses in Region of Hole - Beam No. 2
1 in. = 25.4 mm, 1 ksi. = 6.8976 MPa

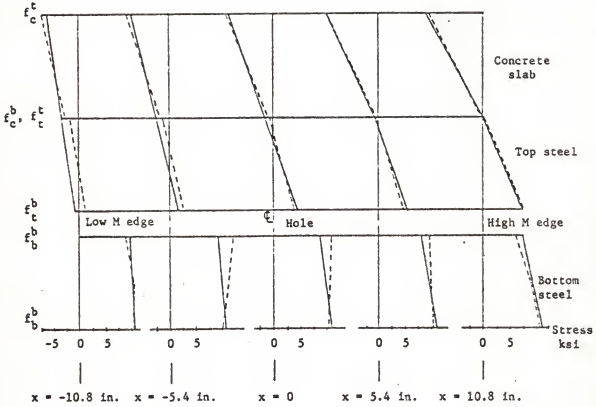

——— Stresses calculated by method of this report

- - - - - - - Stresses obtained from finite element program (3) concrete stresses times ten

Fig. 8 - Longitudinal Stresses in Region of Hole - Beam No. 3
1 in. = 25.4 mm, 1 ksi. = 6.8976 MPa

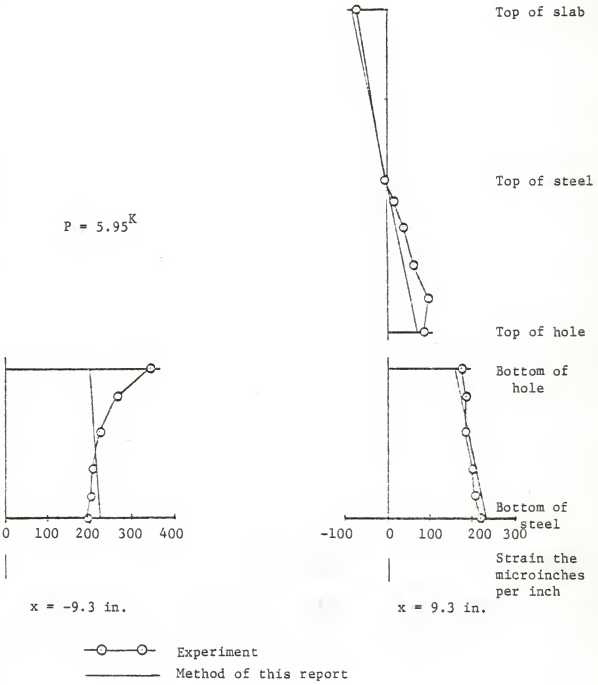

Fig. 9 - Comparison of Strains With Test Results for Beam No. 3 in Region of Hole.
1 in. = 25.4 mm, 1^K = 4.45 KN

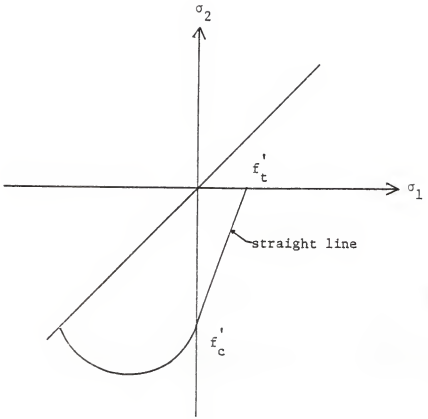

Fig. 10 - Failure State Interaction Diagram for Concrete

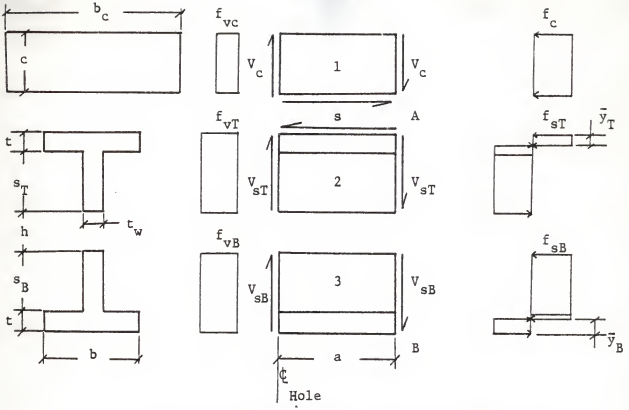

Fig. 11 - Stress Diagram for $M_u = 0$, Model 1, Top Neutral Axis in Steel

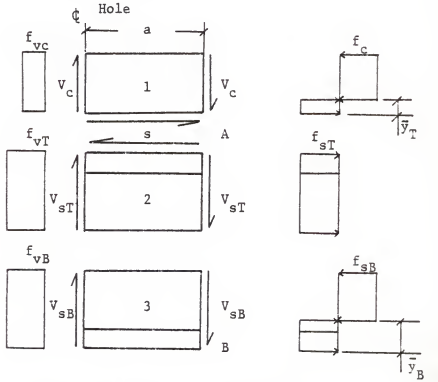

Fig. 12 - Stress Diagram for $M_u = 0$, Model 1, Top Neutral Axis in Concrete

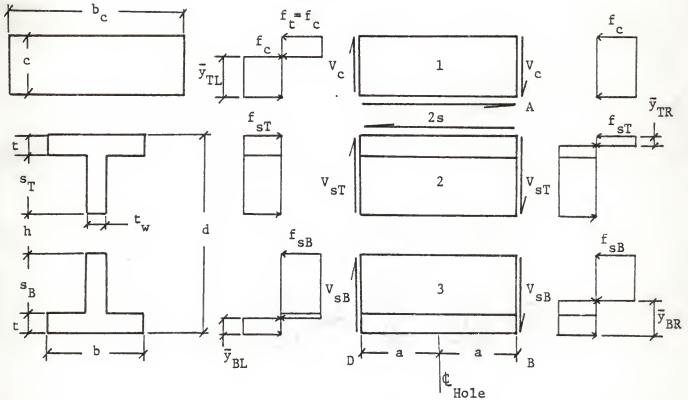

Fig. 13 - Stress Diagram for $M_u \neq 0$, Model 1, Top Right Neutral Axis in Steel

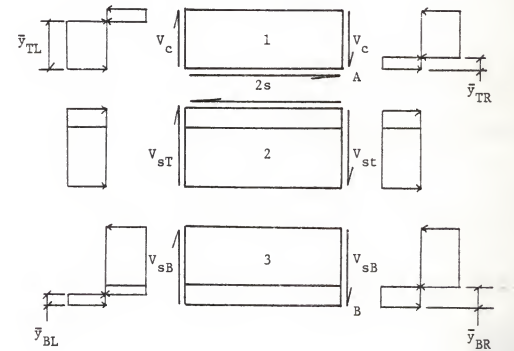

Fig. 14 - Stress Diagram for $M_u \neq 0$, Model 1, Top Right Neutral Axis in Concrete

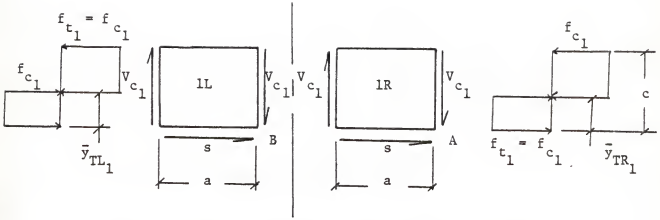

Fig. 15 - State 1 Stresses in Slab for $M_u = 0$, Model 2

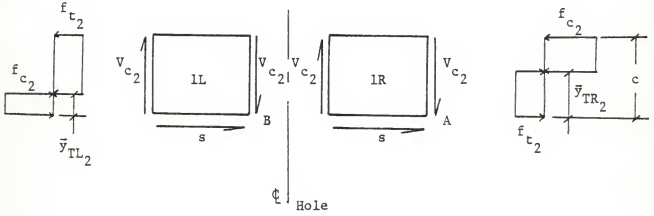

Fig. 16 - State 2 Stresses in Slab for $M_u = 0$, Model 2

Table 1 - Properties of Beams Used in Examples

	Beam No. 1 W14x34	Beam No. 2 W18x45	Beam No. 3 W18x45
b_c, in. (cm)	48 (121.92)	48 (121.92)	48 (121.92)
c, in. (cm)	4 (10.16)	4 (10.16)	4 (10.16)
a, in. (cm)	8 (20.32)	10.8 (27.432)	10.8 (27.432)
h, in. (cm)	8 (20.32)	10.8 (27.432)	10.8 (27.432)
s_T, in. (cm)	2.547 (6.469)	3.031 (7.699)	3.031 (7.699)
s_B, in. (cm)	2.547 (6.469)	3.031 (7.699)	3.031 (7.699)
t, in. (cm)	0.453 (1.151)	0.499 (1.267)	0.499 (1.267)
t_w, in. (cm)	0.287 (0.729)	0.335 (0.851)	0.335 (0.851)
b, in. (cm)	6.75 (17.145)	7.477 (18.991)	7.477 (18.991)
E_s, ksi. (GPa)	29×10^3 (200.03)	29×10^3 (200.03)	29×10^3 (200.03)
E_c, ksi. (GPa)	4.67×10^3 (32.212)	3.87×10^3 (26.694)	3.87×10^3 (26.694)
f'_c, ksi. (MPa)	7.0 (48.283)	4.475 (30.867)	5.81 (40.075)
f'_t, ksi. (MPa)	0.7 (4.828)	0.6745 (4.652)	0.497 (3.428)
f_y, ksi.	35.65 (245.898)	39.5 (272.454)	39.5 (272.454)

Table 2 - Shear Ratios for Example Beams

Beam 1

x, in.	-4	0	+4
% V_T/V	97.1 (90.0)	97.1+ 96.9* (90.3)	97.1+ 96.6* (86.3)
% V_{Tc}/V	87.8 (83.2)	87.8+ 83.2* (83.1)	87.8+ 63.2* (80.7)

+Section uncracked if f_t' from Table 1 used.

*Section cracked if f_t' assumed = 0.

Beam 2

x, ins.	-5.4	0	+5.4
% V_T/V	95.0 (86.7)	95.0 (88.5)	95.0 (86.4)
% V_{Tc}/V	80.5 (81.5)	80.5 (80.4)	80.5 (81.4)

Beam 3

x, ins.	-5.4	0	+5.4
% V_T/V	95.0 (88.4)	95.0 (88.6)	95.0 (86.3)
% V_{Tc}/V	80.5 (84.6)	80.5 (82.2)	80.5 (84.7)

Results from finite element program (3) in parentheses.

```
      $JOB
      C      PROGRAM TO DETERMINE ELASTIC STRESSES IN A COMPOSITE BEAM WITH A HOLE
      C      IF THE SECTION IS CRACKED
      C      THE PROGRAM WILL ALSO DETERMINE VT AND VB ELASTICALLY
1     1000 READ(5,1,END=999) BF,TF,TW,DS,TS,BS,HH
2          1 FORMAT(7F10.3)
3          2 FORMAT(5X,'BF=',F10.3,'TF=',F10.3,'TW=',F10.3,'DS=',F10.3,'TS=',
           1F10.3,/5X,' BS=',F10.3,'HH=',F10.3/)
4           WRITE(6,2) BF,TF,TW,DS,TS,BS,HH
5           READ(5,1) PM,V,XS,EC,XN,XNU,AA
6           READ(5,1) FCPT
7           WRITE(6,3) PM,V,XS,EC,XN,XNU,AA
8          3 FORMAT(5X,'CENTER MOMENT=',F10.3,'TOTAL SHEAR=',F10.3,'XS=',F10.3,
           1'EC=',F10.3,/5X,' XN=',F10.3,'XNU=',F10.3,'AA=',F10.3/)
9           CALL CRST(BF,TF,TW,DS,TS,BS,HH,PM,EC,V,AA,CR,FCT,FCB,FTT,FTB,
           1FBT,FBB,XN,FMT,FMB,FHT,FHB,XNU,XS,FCPT)
10          WRITE(6,4) CR,FCT,FCB,FTT,FTB,FBT,FBB,FMT,FMB
11         4 FORMAT(5X,'CR=',F10.3,'FCT=',F10.3,'FCB=',F10.3,'FTT=',F10.3
           1,'FTB=',F10.3,/5X,' FBT=',F10.3,'FBB=',F10.3,'FMT=',F10.3,'FMB=',
           1F10.3)
12          WRITE(6,5) FHT,FHB
13         5 FORMAT(5X,'FHT=',F10.3,'FHB=',F10.3)
14          GO TO 1000
15       999 STOP
16          END
      C      SUBROUTINE CRST TO COMPUTE CRACKING DEPTH AND STRESSES
17          SUBROUTINE CRST(BF,TF,TW,DS,TS,BS,HH,PM,EC,V,AA,CR,FCT,FCB,FTT,
           1FTB,FBT,FBB,XN,FMT,FMB,FHT,FHB,XNU,XS,FCPT)
18          ST=(DS-HH)/2.-TF
19          SB=ST-EC
20          ST=ST+EC
      C      SECTION PROPERTIES BOTTOM T
21          AB=BF*TF+SB*TW
22          WRITE(6,91) AB
23        91 FORMAT(5X,'Ab=',F10.3)
24          YBB=(SB*TW*(SB/2.+TF)+BF*TF*TF/2.)/AB
25          XIB=SB*TW*(SB*SB/12.+(SB/2.+TF-YBB)**2)+BF*TF*(TF*TF/12.+(YBB-TF
           1/2.)**2)
26          EPS=.001
27          ICO=0
28          ALPH=0.9
29          XKB=AB/XIB**2*(TW/4.*((SB+TF-YBB)**4*SB
           1-2./3.*(SB+TF-YBB)**2*((SB+TF-YBB)**3+(YBB-TF)**3)
           1+1./5.*((SB+TF-YBB)**5+(YBB-TF)**5))+
           1BF/4.*(YBB**4*TF-2./3.*YBB**2*(YBB**3-(YBB-TF)**3)
           1+1./5.*(YBB**5-(YBB-TF)**5)))
30       1000 VT=ALPH*V
31          VB=V-VT
32          TM=VT*XS
33          BM=VB*XS
34          ICOUNT=0
35          IPASS=0
36          CR=TS
      C      SECTION PROPERTIES TOP STEEL T
37          ATS=BF*TF+ST*TW
38          SBB=(ST*TW*(ST/2.+TF)+BF*TF*TF/2.)/ATS
39          XITS=ST*TW*(ST*ST/12.+(ST/2.+TF-SBB)**2)+BF*TF*(TF*TF/12.+(SBB-TF
           1/2.)**2)
      C      SECTION PROPERTIES TOP CCMPOSITE T
```

```
      100 AT=BS*CR+ATS
          WRITE(6,92)AT
       92 FORMAT(5X,'AT=',F10.3)
          YBT=(3S*CR*CR/2.+ATS*(SBB+TS))/AT
          XIT=BS*CR*(CR*CR/12.+(YBT-CR/2.)**2)+XITS+ATS*(SBB+TS-YBT)**2
          WRITE(6,20) CR,YBT,XIT
       20 FORMAT(5X,'CR=',F10.3,'YBT=',F10.3,'XIT=',F10.3)
C         SECTION PROPERTIES COMPOSITE NET SECTION
          XK=DS-YBB+TS
          XM=SBB+TS
          A=AT+AB
          YB=(AB*XK+AT*YBT)/A
          XI=XIB+AB*(XK-YB)**2+XIT+AT*(YB-YBT)**2
          IF(IPASS)1,1,22
C         CHECK STRESS AT TOP AND BOTTOM OF SLAB
        1 FCCR=(-PM*(YB-CR)/XI+TM*(CR-YBT)/XIT)/XN
          FCRC=(-PM*YB/XI-TM*YBT/XIT)/XN
          WRITE(6,19) FCCR,FCRC
       19 FORMAT(5X,'FCCR=',F10.3,'FCRC=',F10.3)
          IPASS=1
       22 IF(FCCR-FCPT)29,2,2
       29 IF(FCRC-FCPT)3,3,900
        2 CR1=(PM*YB/XI+TM*YBT/XIT)/(PM/XI+TM/XIT)
          TEST=ABS((CR-CR1)/CR)
          IF(TEST-EPS)9,9,4
        4 ICOUNT=ICOUNT+1
          CR2=CR
          CR=CR1
          IF(ICOUNT-100)100,100,5
        5 WRITE(6,10) CR2,CR1
       10 FORMAT(5X,'NO CONVERGENCE IN 100 CYCLES CR=',F10.3,'CR1=',F10.3/)
          RETURN
        9 WRITE(6,11) CR,CR1,ICOUNT,ALPH
       11 FORMAT(5X,'CONVERGENCE CR=',F10.3,'CR1=',F10.3,'ICOUNT=',I3,
         1'ALPH=',F10.3)
    3     XKT=BS*AT/(4.*XIT**2)*(YBT***4*CR-2./3.*YBT**2*(YBT**2+(CR-YBT)**3)
         1+1./5.*(YBT**5+(CR-YBT)**5))+
         1BF*AT/(4.*XIT**2)*((TS-YBT+TF)***4*TF-2./3.*(TS-YBT+TF)**2
         1*((TS-YBT+TF)**3
         1-(TS-YBT)**3)+1./5.*((TS-YBT+TF)**5-(TS-YBT)**5))
         1+(TS-YBT+TF+ST/2.)*(ST*TW)*AT/XIT**2*((TS-YBT+TF)**2*TF
         1-1./3.*((TS-YBT+TF)**3-(TS-YBT)**3))
         1+((TS-YBT+TF+ST/2.)*ST*TW)**2*AT*TF/(BF*XIT**2)
         1+TW*AT/(4.*XIT**2)*((TS-YBT+TF+ST)***4*ST-2./3.*(TS-YBT+TF+ST)**2
         1*((TS-YBT+TF+ST)**3-(TS-YBT+TF)**3)
         1+1./5.*((TS-YBT+TF+ST)**5-(TS-YBT+TF)**5))
    3     BETA=(AA**2/(6.*XIB*(1.+XNU))+XKB/AB)/(AA**2/(6.*XIT*(1.+XNU))
         1+XKT/AT)
          ALPH 1=BETA/(1.+BETA)
          TEST=ABS((ALPH-ALPH 1)/ALPH)
          IF(TEST-EPS)33,33,40
       40 ICC=ICC+1
          IF(ICC-100)41,41,42
       41 ALPH=ALPH 1
          GO TO 1000
       42 WRITE(6,12)
       12  FORMAT(5X,'NO CONVERGENCE IN ALPH IN 100 CYCLES')
          RETURN
       33 FCT=(-PM*YB/XI-TM*YBT/XIT)/XN
          FTT=-PM*(YB-TS)/XI+TM*(TS-YBT)/XIT
```

```
      IF(ICOUNT)6,6,7
    6 FCB=FTT/XN
      GO TO 8
    7 FCB=0
    8 FTB=PM*(ST+TF+TS-YB)/XI+TM*(ST+TF+TS-YBT)/XIT
      FBT=PM*(DS+TS-SB-TF-YB)/XI-BM*(SB+TF-YBB)/XIB
      FBB=PM*(DS+TS-YB)/XI+BM*YBB/XIB
       FMT=PM*(TF+TS-YB)/XI+TM*(TF+TS-YBT)/XIT
      FMB=PM*(DS+TS-YB-TF)/XI+BM*(YBB-TF)/XIB
      FHT=(FCT+FCB)*XN*CR*BS/2.+(FTT+ FMT)*TF*BF/2.+( FMT+FTB)*ST*TW/2.
      FHB=(FBT+ FMB)*SB*TW/2.+( FMB+FBB)*TF*BF/2.
      WRITE(6,13)ALPH
   13 FORMAT(5X,'THE RATIO OF VT TO V IS ALPH=',F10.3/)
      GO TO 14
  900 WRITE(6,15)
   15 FORMAT(5X,'ALL CONCRETE CRACKED HENCE CR=0',F10.3/)
C     ALL CONCRETE ASSUMED CRACKED HENCE LOAD CARRIED BY STEEL SECTION ONLY
C     SECTION PROPERTIES AND ELASTIC STRESSES FOR STEEL SECTION
      CR=0
      XKTS=ATS/(XITS**2)*(BF/4.*(SBB**4*TF-2./3.*SBB**2*(SBB**3-
     1(SBB-TF)**3)+(SBB**5-(SBB-TF)**5)/5.)+TW/4.*((TF+ST-SBB)**4+ST
     1-2./3.*(TF+ST-SBB)**2*((SBB-TF)**3+(TF+ST-SBB)**3)
     1+((SBB-TF)**5+(TF+ST-SBB)**5)/5.))
      BETA=(AA**2/(6.*XIB*(1.+XNU))+XKB/AB)
     1/(AA**2/(6.*XITS*(1.+XNU))+XKTS/ATS)
      ALPH=BETA/(1.+BETA)
      WRITE(6,16)ALPH
   16 FORMAT(5X,'THE RATIO OF VT TO V IS ALPH=',F10.3/)
      VT=ALPH*V
      VB=V-VT
      TM=VT*XS
      BM=VB*XS
      YBZ=(AB*(DS-YBB)+ATS*SBB)/(AB+ATS)
      XIZ=XITS+ATS*(YBZ-SBB)**2+XIB+AB*(DS-YBZ-YBB)**2
      FTT=-PM*YBZ/XIZ-TM*SBB/XITS
      FMT=-PM*(YBZ-TF)/XIZ-TM*(SBB-TF)/XITS
      FTB=-PM*(YBZ-TF-ST)/XIZ+TM*(ST+TF-SBB)/XITS
      FBT=PM*(DS-YBZ-SB-TF)/XIZ-BM*(SB+TF-YBB)/XIB
      FMB=PM*(DS-YBZ-TF)/XIZ+BM*(YBB-TF)/XIB
      FBB=PM*(DS-YBZ)/XIZ+BM*YBB/XIB
      FHT=(FTT+FMT)*TF*BF/2.+(FMT+FTB)*ST*TW/2.
      FHB=(FBT+FMB)*SB*TW/2.+(FMB+FBB)*TF*BF/2.
      FCT=0
      FCB=0
   14 RETURN
      END

     $ENTRY
BF=     6.750TF=     0.453TW=     0.287DS=    14.000TS=     4.000
 BS=     7.729HH=     8.000

CENTER MOMENT=   420.000TOTAL SHEAR=     5.000XS=    -8.000EC=     0.000
 XN=     6.210XNU=     0.300AA=     8.000

AB=     3.789
AT=    34.705
CR=     4.000YBT=     2.275XIT=    64.360
FCCR=    -0.137FCRC=    -0.093
AT=    34.705
CR=     4.000YBT=     2.275XIT=    64.360
```

```
FCCR=     -0.150FCRC=     -0.077
THE RATIO OF VT TO V IS ALPH=      0.971

CR=       4.000FCT=     -0.077FCB=     -0.150FTT=     -0.929FTB=     -1.268
 FBT=       7.128FBB=       6.642FMT=      -0.980FMB=       6.715
FHT=    -25.482FHB=     25.482
BF=       6.750TF=       0.453TW=       0.287DS=      14.000TS=       4.000
 BS=       7.729HH=       8.000

CENTER MOMENT=    420.000TOTAL SHEAR=       5.000XS=     -4.000EC=       0.000
 XN=       6.210XNU=       0.300AA=       8.000

AB=       3.789
AT=      34.705
CR=       4.000YBT=       2.275XIT=      64.360
FCCR=     -0.060FCRC=     -0.195
AT=      34.705
CR=       4.000YBT=       2.275XIT=      64.360
FCCR=     -0.066FCRC=     -0.187
THE RATIO OF VT TO V IS ALPH=      0.971

CR=       4.000FCT=     -0.187FCB=     -0.066FTT=     -0.409FTB=       0.158
 FBT=       6.818FBB=       6.810FMT=      -0.323FMB=       6.736
FHT=    -25.482FHB=     25.482
BF=       6.750TF=       0.453TW=       0.287DS=      14.000TS=       4.000
 BS=       7.729HH=       8.000

CENTER MOMENT=    420.000TOTAL SHEAR=       5.000XS=       0.000EC=       0.000
 XN=       6.210XNU=       0.300AA=       8.000

AB=       3.789
AT=      34.705
CR=       4.000YBT=       2.275XIT=      64.360
FCCR=      0.018FCRC=     -0.298
AT=      32.940
CR=       3.772YBT=       2.188XIT=      59.525
AT=      32.897
CR=       3.766YBT=       2.186XIT=      59.419
CONVERGENCE CR=      3.766CR1=       3.766ICOUNT=  2ALPH=       0.900
AT=      34.705
CR=       4.000YBT=       2.275XIT=      64.360
FCCR=      0.018FCRC=     -0.298
AT=      32.940
CR=       3.772YBT=       2.188XIT=      59.525
AT=      32.897
CR=       3.766YBT=       2.186XIT=      59.419
CONVERGENCE CR=      3.766CR1=       3.766ICOUNT=  2ALPH=       0.965
THE RATIO OF VT TO V IS ALPH=      0.969

CR=       3.766FCT=     -0.297FCB=       0.000FTT=       0.115FTB=       1.586
 FBT=       5.510FBB=       6.982FMT=       0.337FMB=       6.759
FHT=    -25.493FHB=     25.493
BF=       6.750TF=       0.453TW=       0.287DS=      14.000TS=       4.000
 BS=       7.729HH=       8.000

CENTER MOMENT=    420.000TOTAL SHEAR=       5.000XS=       4.000EC=       0.000
 XN=       6.210XNU=       0.300AA=       8.000

AB=       3.789
AT=      34.705
```

```
CR=     4.000YBT=      2.275XIT=     64.360
FCCR=     0.096FCRC=     -0.400
AT=    28.738
CR=     3.228YBT=      1.997XIT=     51.138
AT=    27.340
CR=     3.047YBT=      1.938XIT=     49.221
AT=    27.152
CR=     3.023YBT=      1.931XIT=     48.993
CONVERGENCE CR=     3.023CR1=      3.020ICOUNT=   3ALPH=      0.900
AT=    34.705
CR=     4.000YBT=      2.275XIT=     64.360
FCCR=     0.101FCRC=     -0.408
AT=    28.548
CR=     3.203YBT=      1.988XIT=     50.854
AT=    27.069
CR=     3.012YBT=      1.927XIT=     48.895
AT=    26.868
CR=     2.986YBT=      1.919XIT=     48.663
CONVERGENCE CR=     2.986CR1=      2.983ICOUNT=   3ALPH=      0.966
THE RATIO OF VT TO V IS ALPH=      0.966

CR=     2.986FCT=     -0.427FCB=      0.000FTT=      0.903FTB=      3.567
 FBT=     4.517FBB=      7.156FMT=      1.305FMB=      6.757
FHT=   -25.42OFHB=     25.392
BF=     6.750TF=      0.453TW=      0.287OS=     14.000TS=      4.000
 BS=     7.729HH=      8.000

CENTER MOMENT=   420.000TOTAL SHEAR=      5.000XS=      8.000EC=      0.000
 XN=     6.210XNU=      0.300AA=      8.000

AB=     3.789
AT=    34.705
CR=     4.000YBT=      2.275XIT=     64.360
FCCR=     0.173FCRC=     -0.503
AT=    26.775
CR=     2.974YBT=      1.916XIT=     48.558
AT=    24.540
CR=     2.685YBT=      1.832XIT=     46.505
AT=    24.244
CR=     2.647YBT=      1.822XIT=     46.298
AT=    24.221
CR=     2.644YBT=      1.821XIT=     46.282
CONVERGENCE CR=     2.644CR1=      2.643ICOUNT=   4ALPH=      0.900
AT=    34.705
CR=     4.000YBT=      2.275XIT=     64.360
FCCR=     0.185FCRC=     -0.517
AT=    26.576
CR=     2.948YBT=      1.908XIT=     48.338
AT=    24.258
CR=     2.648YBT=      1.823XIT=     46.307
AT=    23.955
CR=     2.609YBT=      1.812XIT=     46.108
AT=    23.932
CR=     2.606YBT=      1.812XIT=     46.093
CONVERGENCE CR=     2.606CR1=      2.606ICOUNT=   4ALPH=      0.965
THE RATIO OF VT TO V IS ALPH=      0.965

CR=     2.606FCT=     -0.558FCB=      0.000FTT=      1.855FTB=      5.846
 FBT=     3.467FBB=      7.342FMT=      2.457FMB=      6.757
FHT=   -25.295FHB=     25.292
```

```
BF=      7.477TF=      0.499TW=      0.335DS=     17.860TS=      4.000   62
 BS=      6.410HH=     10.800

CENTER MOMENT=    494.100TOTAL SHEAR=      4.575XS=    -10.800EC=      0.000
 XN=      7.490XNU=      0.280AA=     10.800

AB=      4.746
AT=     30.386
CR=      4.000YBT=      2.410XIT=     65.169
FCCR=     -0.186FCRC=      0.005
AT=     30.386
CR=      4.000YBT=      2.410XIT=     65.169
FCCR=     -0.194FCRC=      0.017
THE RATIO OF VT TO V IS ALPH=      0.950

CR=      4.000FCT=      0.017FCB=     -0.194FTT=     -1.454FTB=     -2.850
 FBT=      6.505FBB=      5.018FMT=     -1.651FMB=      5.228
FHT=    -25.070FHB=     25.070
BF=      7.477TF=      0.499TW=      0.335DS=     17.860TS=      4.000
 BS=      6.410HH=     10.800

CENTER MOMENT=    494.100TOTAL SHEAR=      4.575XS=     -5.400EC=      0.000
 XN=      7.490XNU=      0.280AA=     10.800

AB=      4.746
AT=     30.386
CR=      4.000YBT=      2.410XIT=     65.169
FCCR=     -0.114FCRC=     -0.105
AT=     30.386
CR=      4.000YBT=      2.410XIT=     65.169
FCCR=     -0.118FCRC=     -0.099
THE RATIO OF VT TO V IS ALPH=      0.950

CR=      4.000FCT=     -0.099FCB=     -0.118FTT=     -0.882FTB=     -1.007
 FBT=      5.422FBB=      5.251FMT=     -0.899FMB=      5.276
FHT=    -25.070FHB=     25.070
BF=      7.477TF=      0.499TW=      0.335DS=     17.860TS=      4.000
 BS=      6.410HH=     10.800

CENTER MOMENT=    494.100TOTAL SHEAR=      4.575XS=      0.000EC=      0.000
 XN=      7.490XNU=      0.280AA=     10.800

AB=      4.746
AT=     30.386
CR=      4.000YBT=      2.410XIT=     65.169
FCCR=     -0.041FCRC=     -0.215
AT=     30.386
CR=      4.000YBT=      2.410XIT=     65.169
FCCR=     -0.041FCRC=     -0.215
THE RATIO OF VT TO V IS ALPH=      0.950

CR=      4.000FCT=     -0.215FCB=     -0.041FTT=     -0.309FTB=      0.836
 FBT=      4.340FBB=      5.485FMT=     -0.147FMB=      5.323
FHT=    -25.070FHB=     25.070
BF=      7.477TF=      0.499TW=      0.335DS=     17.860TS=      4.000
 BS=      6.410HH=     10.800

CENTER MOMENT=    494.100TOTAL SHEAR=      4.575XS=      5.400EC=      0.000
 XN=      7.490XNU=      0.280AA=     10.800
```

```
AB=      4.746
AT=     30.386
CR=      4.000YBT=      2.410XIT=     65.169
FCCR=    0.031FCRC=    -0.324
AT=     30.386
CR=      4.000YBT=      2.410XIT=     65.169
FCCR=    0.035FCRC=    -0.330
THE RATIO OF VT TO V IS ALPH=      0.950

CR=      4.000FCT=     -0.330FCB=      0.035FTT=      0.263FTB=      2.079
 FBT=    3.258FBB=      5.719FMT=      0.604FMB=      5.371
FHT=   -25.070FHB=     25.070
BF=      7.477TF=      0.499TW=       0.335DS=      17.860TS=      4.000
 BS=     6.410HH=      10.800

CENTER MOMENT=    494.100TOTAL SHEAR=      4.575XS=      10.800EC=      0.000
 XN=      7.490XNU=      0.280AA=      10.800

AB=      4.746
AT=     30.386
CR=      4.000YBT=      2.410XIT=     65.169
FCCR=    0.104FCRC=    -0.434
AT=     30.386
CR=      4.000YBT=      2.410XIT=     65.169
FCCR=    0.112FCRC=    -0.446
THE RATIO OF VT TO V IS ALPH=      0.950

CR=      4.000FCT=     -0.446FCB=      0.112FTT=      0.835FTB=      4.522
 FBT=    2.175FBB=      5.953FMT=      1.356FMB=      5.419
FHT=   -25.070FHB=     25.070
BF=      7.477TF=      0.499TW=       0.335DS=      17.860TS=      4.000
 BS=     6.410HH=      10.800

CENTER MOMENT=    792.000TOTAL SHEAR=      2.000XS=     -10.800EC=      0.000
 XN=      7.490XNU=      0.280AA=      10.800

AB=      4.746
AT=     30.386
CR=      4.000YBT=      2.410XIT=     65.169
FCCR=   -0.129FCRC=    -0.248
AT=     30.386
CR=      4.000YBT=      2.410XIT=     65.169
FCCR=   -0.133FCRC=    -0.243
THE RATIO OF VT TO V IS ALPH=      0.950

CR=      4.000FCT=     -0.243FCB=     -0.133FTT=     -0.996FTB=     -0.271
 FBT=    7.903FBB=      8.588FMT=     -0.894FMB=      8.491
FHT=   -40.184FHB=     40.184
BF=      7.477TF=      0.499TW=       0.335DS=      17.860TS=      4.000
 BS=     6.410HH=      10.800

CENTER MOMENT=    792.000TOTAL SHEAR=      2.000XS=     -5.400EC=      0.000
 XN=      7.490XNU=      0.280AA=      10.800

AB=      4.746
AT=     30.386
CR=      4.000YBT=      2.410XIT=     65.169
FCCR=   -0.298FCRC=    -0.296
AT=     30.386
CR=      4.000YBT=      2.410XIT=     65.169
```

```
FCCR=    -0.100FCRC=    -0.293
THE RATIO OF VT TO V IS ALPH=      0.950

CR=      4.000FCT=     -0.293FCB=     -0.100FTT=     -0.746FTB=      0.534
 FBT=    7.430FBB=      8.690FMT=     -0.565FMB=      8.512
FHT=    -40.184FHB=    40.184
BF=      7.477TF=      0.499TW=       0.335DS=      17.860TS=       4.000
 BS=     6.410HH=      10.800

CENTER MOMENT=   792.000TOTAL SHEAR=      2.000XS=       0.000EC=       0.000
 XN=     7.490XNU=      0.280AA=       10.800

AB=      4.746
AT=     30.386
CR=      4.000YBT=      2.410XIT=      65.169
FCCR=    -0.066FCRC=    -0.344
AT=     30.386
CR=      4.000YBT=      2.410XIT=      65.169
FCCR=    -0.066FCRC=    -0.344
THE RATIO OF VT TO V IS ALPH=      0.950

CR=      4.000FCT=     -0.344FCB=     -0.066FTT=     -0.496FTB=      1.340
 FBT=    6.957FBB=      8.792FMT=     -0.236FMB=      8.533
FHT=    -40.184FHB=    40.184
BF=      7.477TF=      0.499TW=       0.335DS=      17.860TS=       4.000
 BS=     6.410HH=      10.800

CENTER MOMENT=   792.000TOTAL SHEAR=      2.000XS=       5.400EC=       0.000
 XN=     7.490XNU=      0.280AA=       10.800

AB=      4.746
AT=     30.386
CR=      4.000YBT=      2.410XIT=      65.169
FCCR=    -0.035FCRC=    -0.392
AT=     30.386
CR=      4.000YBT=      2.410XIT=      65.169
FCCR=    -0.033FCRC=    -0.395
THE RATIO OF VT TO V IS ALPH=      0.950

CR=      4.000FCT=     -0.395FCB=     -0.033FTT=     -0.246FTB=      2.146
 FBT=    6.483FBB=      8.895FMT=      0.092FMB=      8.554
FHT=    -40.184FHB=    40.184
BF=      7.477TF=      0.499TW=       0.335DS=      17.860TS=       4.000
 BS=     6.410HH=      10.800

CENTER MOMENT=   792.000TOTAL SHEAR=      2.000XS=      10.800EC=       0.000
 XN=     7.490XNU=      0.280AA=       10.800

AB=      4.746
AT=     30.386
CR=      4.000YBT=      2.410XIT=      65.169
FCCR=    -0.003FCRC=    -0.440
AT=     30.386
CR=      4.000YBT=      2.410XIT=      65.169
FCCR=    -0.001FCRC=    -0.445
AT=     30.351
CR=      3.995YBT=      2.409XIT=      65.080
CONVERGENCE CR=     3.995CR1=      3.994ICOUNT=  1ALPH=       0.950
THE RATIO OF VT TO V IS ALPH=      0.950
```

```
CR=      3.995FCT=    -0.445FCB=      0.000FTT=      0.005FTB=      2.954
 FBT=      6.010FBB=      8.997FMT=      0.422FMB=      8.574
FMT=    -40.192FMB=     40.183

CORE USAGE       OBJECT CODE=    10896 BYTES,ARRAY AREA=        0 BYTES,TOTAL AREA AV,

DIAGNOSTICS        NUMBER OF ERRORS=        0, NUMBER OF WARNINGS=        0, NUMBER OF

COMPILE TIME=      0.56 SEC,EXECUTION TIME=      0.99 SEC,      22.04.43    WEDNESDAY
```

BEHAVIOR OF COMPOSITE BEAMS WITH WEB OPENINGS

by

KRIGO S. ELIUFOO

B.S., Kansas State University, 1978

AN ABSTRACT OF A MASTER'S THESIS

submitted in partial fulfillment of the

requirements for the degree

MASTER OF SCIENCE

Department of Civil Engineering

KANSAS STATE UNIVERSITY
Manhattan, Kansas

1979

ABSTRACT

A method of analysis and solution technique have been developed for determining the stresses in the elastic level and shear forces in the regions of web openings in steel-concrete composite beams. Reasonable agreement was achieved when results obtained by the method developed here were compared to results from a finite element program (3). The Vierendeel approach was used in developing the method of elastic analysis presented in this thesis. A general method of approach to the ultimate strength analysis was also developed and discussed.